Scientific Reports

https://doi.org/10.1038/s41598-026-39536-x

Article in Press

A deep neural network model for heat transfer in darcy–forchheimer hybrid nanofluid flow with activation energy

Received: 28 November 2025

Accepted: 5 February 2026

Published online: 11 February 2026

Cite this article as: Ayman-Mursaleen M., Saeed S.T., Almohammadi S.M. *et al.* A deep neural network model for heat transfer in darcy–forchheimer hybrid nanofluid flow with activation energy. *Sci Rep* (2026). https://doi.org/10.1038/s41598-026-39536-x

Mohammad Ayman-Mursaleen, Syed Tauseef Saeed, Saja Mohammad Almohammadi, Khalid Arif & Muhammad Imran

We are providing an unedited version of this manuscript to give early access to its findings. Before final publication, the manuscript will undergo further editing. Please note there may be errors present which affect the content, and all legal disclaimers apply.

If this paper is publishing under a Transparent Peer Review model then Peer Review reports will publish with the final article.

ARTICLE IN PRESS

© The Author(s) 2026. **Open Access** This article is licensed under a Creative Commons Attribution-NonCommercial-NoDerivatives 4.0 International License, which permits any non-commercial use, sharing, distribution and reproduction in any medium or format, as long as you give appropriate credit to the original author(s) and the source, provide a link to the Creative Commons licence, and indicate if you modified the licensed material. You do not have permission under this licence to share adapted material derived from this article or parts of it. The images or other third party material in this article are included in the article's Creative Commons licence, unless indicated otherwise in a credit line to the material. If material is not included in the article's Creative Commons licence and your intended use is not permitted by statutory regulation or exceeds the permitted use, you will need to obtain permission directly from the copyright holder. To view a copy of this licence, visit http://creativecommons.org/licenses/by-nc-nd/4.0/.

ARTICLE IN PRESS

A Deep Neural Network Model for Heat Transfer in Darcy–Forchheimer Hybrid Nanofluid Flow with Activation Energy

Mohammad Ayman-Mursaleen[1], Syed Tauseef Saeed[2,*], Saja Mohammad Almohammadi[3], Khalid Arif[2], Muhammad Imran[4]

[1]Department of Mathematics, Faculty of Science, University of Ostrava, Mlýnská 702/5, 702 00 Ostrava, Czechia.

[2]Department of Mathematics and Statistics, The University of Lahore, Lahore, Pakistan.

[3]Department of Mathematics, King Khalid University, Abha, Saudi Arabia.

[4]Department of Mathematics, Northwestern polytechnical University, China.

*Corresponding Author: tauseef.saeed@math.uol.edu.pk

Abstract

This paper investigates the magnetohydrodynamic (MHD) flow along with heat and mass transfer behavior of Casson-type hybrid nanofluid through aluminum oxide (Al_2O_3) as well as titanium dioxide (TiO_2) nanoparticles dispersed throughout engine oil, a thermally stable functioning fluid that is used in utmost industrialized thermal exchanger applications. The advanced model incorporates the collective influences of heat radiation, Darcy–Forchheimer permeable media resistance, magnetic field-heating, and activation energy under nonlinear chemical reaction circumstances. Employing similarity transformations, the intricate governing equations are streamlined to ordinary differential equations (ODEs) that are numerically solved by means of the Bvp4c solver. The numerical solutions attained via the Bvp4c algorithm are employed for training a Morlet Wavelet Neural Network with Particle Swarm Optimization as well as Neural Network Algorithm (MWNN–PSO–NNA), through improving prediction robustness as well as generality behavior. The results show that strengthening the magnetic field leads to a decrease in the velocity distribution whereas thermal radiation growth in temperature, via variations falling within the range of 15–25% across the flow domain. Raising activation energy nearly 30% is observed to regulate species concentration as well as promote a more controlled thermal response inside the porous structure. In comparison with the base fluid and single-nanoparticle suspensions, the hybrid nanofluid exhibits superior thermal performance. Moreover, the MWNN–PSO–NNA outcomes remain in close agreement with the numerical solutions, yielding error levels of the order 10□□–10□□, which confirms the reliability of the proposed framework for complex non-Newtonian hybrid nanofluid

ARTICLE IN PRESS

systems relevant to industrial thermal applications. The proposed neural network model demonstrates strong predictive capability, achieving an accuracy greater than 99% while reducing computational time by approximately 45% when compared with traditional numerical methods. An ANN is developed to rapidly predict flow, heat, and mass transfer. Trained on bvp4c data, it achieves comparable accuracy while reducing computational time by 45% compared to repeated numerical simulations. Additionally, the hybrid nanofluid formulation displays strong potential for industrial lubrication applications, thermal control of mechanical components, and energy-based cooling systems, where improved heat transfer productivity is a main performance requirement. The main motivation of this study is to address the growing demand for efficient thermal management in industrial lubrication systems involving non-Newtonian fluids. The goal is to apply a robust MWNN–PSO–NNA framework to accurately predict the flow, heat, and mass transfer characteristics of Casson hybrid nanofluid over a radially stretching surface under combined physical effects. This study is the first to integrate engine-oil-based Casson hybrid nanofluid modeling with Darcy–Forchheimer porous effects and an optimized MWNN–PSO–NNA framework, providing highly accurate thermal–fluid predictions relevant to advanced industrial heat transfer systems.

Keywords: Casson Hybrid nanofluid; Thermal radiation; Chemical reaction; Activation energy; Engine oil; Darcy–Forchheimer porous medium; Artificial Neural Network (ANN)

Nomenclature

Symbol	Description with S.I. Unit
	Roman Symbols
u, v	Velocity components along x- and y-directions (m/s)
T	Fluid temperature (K)
T_w	Wall temperature (K)
T_∞	Ambient temperature (K)
C	Nanoparticle concentration (kg/m³)
C_w	Wall concentration (kg/m³)
C_∞	Ambient concentration (kg/m³)
ρ	Density of fluid or nanofluid (kg/m³)
μ	Dynamic viscosity (Pa·s)
ν	Kinematic viscosity (m²/s)
k	Thermal conductivity (W/m·K)
C_p	Specific heat capacity at constant pressure (J/kg·K)
α	Thermal diffusivity (m²/s)
D_B	Brownian diffusion coefficient (m²/s)
D_T	Thermophoresis diffusion coefficient (m²/s)

ARTICLE IN PRESS

B_0	Magnetic Field Strength T(Tesla)
R	Universal gas constant (J/mol. K)
σ	Electrical conductivity (S/m.($\Omega^{-1}\cdot m^{-1}$))
ϕ	Nano-particles volume fractions
q_r	Radiative heat flux (W/m²)
σ^*	Stefan–Boltzmann constant
k^*	Mean absorption coefficient
h_f	Convective heat transfer coefficient (W m^{-2} K^{-1})
Dimensionless Variable	
ψ	Dimensionless stream function
$\theta(\eta)$	Dimensionless temperature
$\phi(\eta)$	Dimensionless concentration
η	Similarity variable
Dimensionless Parameter	
β	Casson fluid parameter
n	Nonlinearity index (power-law index)
M	Magnetic field parameter
K	Permeability parameter
Fr	Forchheimer (inertial drag) number
λ	Velocity slip parameter
Ec	Eckert number (viscous dissipation parameter)
Pr	Prandtl number
R_d	Thermal radiation parameter
Q^*	Heat source
Nb	Heat generation due to nanoparticle concentration
M_1	Magnetic heating parameter
Sc	Schmidt number
K_r	Chemical reaction rate constant
E_1	Activation energy parameter
γ	Temperature-dependent activation modifier
Re	Reynolds number
δ	Heat source/sink parameter
M_2	Magnetic energy coefficient
Hybrid Nanofluid Properties	
k_{hnf}	Convective heat transfer coefficient (W/m^2 K)
μ_{hnf}	Dynamic viscosity of Hybrid nanofluid (PaS)
σ_{hnf}	Electrical conductivity of Hybrid nanofluid ($\Omega^{-1}m^{-1}$)
ρ_{hnf}	Density of Hybrid nanofluid (Kg m^{-3})
Machine Learning and Optimization Symbols	
ψ_m	Morlet wavelet function
W	Neural network weight vector
$E(T)$	Fitness function
P_{LB},P_{GB}	PSO personal and global best positions
w	Inertia weight (in PSO)
c_1, c_2	Acceleration coefficients (PSO)

ARTICLE IN PRESS

ARTICLE IN PRESS

u_1, u_2	Random numbers uniformly distributed in [0, 1]
T_{MWNN}	MWNN-predicted temperature

1. Introduction

The growing need for industrial systems to move heat and mass quickly, like porous catalytic beds, lubrication channels, and electromagnetic cooling devices, has made the need for high-performance thermal fluids even greater. Water, ethylene glycol, and kerosene oil are common base fluids, but they don't work well when the temperature is high because they don't conduct heat well and don't stay stable. As a result, hybrid nanofluids, which hold more than one type of nanoparticle in a suitable base fluid, have become promising alternatives because they have better thermophysical properties and can be adjusted to work better. Ghobadi and Hassankolaei [1] numerically examined the magnetohydrodynamic (MHD) flow of Al_2O_3 - TiO_2/water hybrid nanofluids along a stretching cylindrical surface with the emphasis on the nanoparticle shape factor effect on flow and thermal transport behavior. Their findings indicated that the heat transfer rate in hybrid nanofluids was much higher compared to suspensions of single nanoparticles, showing sensitivity to particle shape. The research proved that the integration of metal oxide nanoparticles under conditions of MHD had the potential to maximize boundary layer flow behavior and thermal gradients, which in the context of industrial systems needs high thermal conductivity and magnetic control [2]. Based on such foundational research, the current work includes a Casson fluid model with engine oil as the base fluid and is subject to Darcy–Forchheimer drag, activation energy, and radiation effects and broadens the applicability to more real-world industrial and porous media conditions with the help of sophisticated neural network–based solvers [3].

Al_2O_3 and TiO_2 nanoparticles were chosen for their high thermal conductivity, strong chemical stability, and common use in industrial heat transfer systems. Incorporating both into the hybrid nanofluid improves heat transfer efficiency while remaining compatible with the engine oil base fluid. The Casson fluid model is a good way to describe yield stress and shear-thinning behavior that is often seen in paints, lubricants, and polymers that are not Newtonian fluids. When used as a base for nanofluids, engine oil stays stable in terms of temperature and flow. It can handle high operating temperatures (over 300 °C) and keeps nanoparticles suspended well without the need for surfactants. Current experimental examination directed in [4] discovered that a hybrid Al_2O_3 - TiO_2 nanofluid in SAE 5W30 engine oil got a heat conductivity enrichment of up to 8.6% at 100□°C, keeping stable

ARTICLE IN PRESS

nanoparticle diffusion all through heat cycling.

Titanium dioxide (TiO_2) and aluminum oxide (Al_2O_3) nanoparticles are widely investigated as effective additives in engine oil because of their superior mechanical strength, chemical stability, and resistance to high operating temperatures. When dispersed in lubricating oil, these nanoparticles enhance tribological behavior by minimizing frictional losses and surface wear between moving engine components. Their small size enables them to penetrate contact interfaces, where they assist in surface smoothing, rolling effects, and the formation of stable protective layers. As a result, TiO_2 and Al_2O_3-induced nano-lubricants contribute to improved engine efficiency, better thermal performance, and increased service life of mechanical systems [5–7].

These results suggest that the approach could be beneficial in industrial heat-transfer systems involving porous media, thermal radiation, and magnetic heating. Due to its stress through yield as well as shear-thinning behavior, the Casson fluid has developed a standard non-Newtonian fluid model for capturing the features of manufacturing lubricants along with polymeric fluids. Higher heat systems within applications for instance lubrication channels, extrusion cooling, catalytic flow beds are through possible by its amalgamation with hybrid nanofluids. For its greater viscosity, intrinsic lubricating features, thermal permanency (above 300°C), as well as consistency through nanoparticle suspension, engine oil mostly has stored a lot of interest by means of a base fluid [8 – 10].

Recent studies have applied ANN-based models to predict thermal transport in hybrid and penta-hybrid nanofluids. Kumar et al. [11] used deep neural networks with a finite difference approach to study blood-based penta-hybrid nanofluid flow in fin geometries, while optimizing and classifying thermal transport in ternary hybrid nanofluid flows over convective surfaces was focused in [12]. These studies demonstrate the capability of ANN models to capture complex nanofluid behavior accurately.

In order to model the inertial and permeability-driven resistive forces in such porous media, Darcy–Forchheimer drag must be included. Forchheimer resistance significantly reduces velocity while increasing heat generation in high-viscosity fluids, according to Paul et al. [13] investigation of Casson tri-hybrid nanofluids over porous rotating discs. Numerous systems function in radiative environments or electromagnetic fields, where boundary layer dynamics are influenced by thermal radiation and magnetic field effects (MHD). By simulating engine oil-based Casson nanofluids under

ARTICLE IN PRESS

shrinking sheet conditions. Ayman-Mursaleen [14] verified that the quadratic function preserving wavelet type Baskakov operators for enhanced function approximation. Also, the traditional numerical solvers frequently need fine discretization, guess-based iteration, and high computational costs to solve the resulting system of highly nonlinear and coupled partial differential equations [15]. Artificial Neural Networks (ANNs), on the other hand, have become a potent substitute because of their capacity to simulate intricate, nonlinear mappings without the need for mesh creation [16-18].

Artificial Neural Networks (ANNs) have developed progressively operational tools in modern years used for simulating the nonlinear behavior of nanofluids which is used in manufacturing lubrication as well as heat management. After using on intricate fluid structures such as hybrid nano-lubricants, these techniques based on data offer higher extrapolative exactness as compared to traditional correlations. In the evolution of progressive nanofluids for the industrial sectors, automotive, and energy where correct viscosity regulator is needed used for system productivity along with consistency [19]. Hence these investigations point out the mounting implication of simulation through ANN. These expansions help by means of the motivation for the present research that observes the MHD flow of a Casson hybrid nanofluid through Al_2O_3 and TiO_2 nanoparticles within engine oil via stretching surface within a Darcy–Forchheimer permeable media although accounting for the effects of heat radiation, magnetic heating, and activation energy.

Non-Newtonian hybrid nanofluids have attracted increasing interest because of their superior heat transfer capability in modern energy systems, lubrication technologies, and chemical processing applications. Casson hybrid nanofluids are particularly suitable for representing yield-stress fluids commonly encountered in industrial suspensions, surface coatings, and bio-inspired engineering materials [20]. The interaction of magnetic fields, porous medium resistance, thermal radiation, and chemically reactive effects plays a crucial role in modifying the fluid's momentum, thermal, and mass transport behavior. A comprehensive understanding of these coupled physical mechanisms is therefore vital for improving thermal efficiency and achieving effective control of transport processes in advanced heat transfer and manufacturing applications [21].

The modern investigations highlight the significance of interfacial nano-layers, Marangoni convection, with nonlinear impacts in refining hybrid nanofluid heat as well as mass transmission. Mohanty et al. [22] considered GO–MoS□/water hybrid nanofluid across a stretched sheet under an inclined magnetic field. Interfacial nano-layer effects on reactive with Darcy–Forchheimer Casson

ARTICLE IN PRESS

hybrid nanofluid flows had been examined by Mohanty et al. [23]. Furthermore, thermo-solutal Marangoni convective bio-hybrid nanofluid flow [24] and radiative cross-ternary hybrid nanofluid flow [25] emphasized improvements in thermal behavior and concentrated irreversibility.

Existing studies have inspected thermal behavior with entropy in intricate nanofluid networks under porous effects, radiative, and magnetic. Jameel et al. [26] considered nonlinear radiative Sutter by nanofluid flow using Hall effects with activation energy, whereas Baithalu et al. [27] examined entropy generation in magnetized blood-based hybrid nanofluid between parallel disks. Kumar et al. [28] investigated third-grade nanofluid flow with double diffusion through stretched Riga plate. Kaswan et al. [29] inspected heating transmission in hybrid AA7072/AA7075 alloy nanofluids under MHD Darcy–Forchheimer flow. Agrawal et al. [30] inspected bi-directional Williamson micropolar fluid in permeable medium using activation energy as well as thermal radiation. Overall, such researches emphasize the interaction of nanofluid composition, magnetic fields, and non-Newtonian effects upon heat with mass transfer.

Current researches have comprehensively examined modern nanofluid algorithms to improve heat as well as mass transfer under intricate physical effects. Panda et al. [31] studied Arrhenius activation energy influences on multi-phase nanofluid flow through convective boundaries, emphasizing its sensitivity for heat transmission optimization. Shamshuddin et al. [32] analyzed electromagnetic radiative tri-hybrid nanofluid flow in bi-directional stretched schemes, indicating significant thermal improvement within the permeable medium. Irreversibility and Entropy generation in MHD Williamson fluid flow via inclined networks had been indicated in [33], signifying the impact of magnetic effects over network productivity.

Recent studies have highlighted the importance of combining complex physical mechanisms with advanced numerical and machine-learning approaches in nanofluid research. Nabwey et al. [34] investigated entropy generation in MHD hybrid nanofluid flow within a porous square cavity containing geometric obstructions, emphasizing the role of magnetic and thermal effects on irreversibility. A two-phase Carreau bio-magnetic hybrid nanofluid over an inclined spinning disk using numerical simulations coupled with machine learning techniques was analyzed to enhance predictive accuracy [35]. In a related work, Jakeer et al. [36] examined the combined influence of activation energy and Coriolis force on three-dimensional dusty nanofluid flow with gyrotactic microorganisms, employing a hybrid numerical–machine learning framework to capture the

ARTICLE IN PRESS

underlying transport phenomena.

This expanding overlap between ANN-based prediction and physical modelling is extremely pertinent to your current research. Using engine oil, Awais et al. [37] studied hybrid nanofluids in a trapezium cavity and verified a significant increase in heat transfer under geometric and convective effects, which is directly consistent with porous industrial geometries. Similar to this, Sarma & Paul [38] investigated Casson hybrid nanofluid flow in engine oil with activation energy and suction effects, confirming the function of nanoparticle blending in mass diffusion regulation and boundary layer control. To the best of our knowledge, this study is the first to investigate the flow with thermal behavior of Casson hybrid nanofluid (Al_2O_3 - TiO_2/engine oil) across a radially stretched surface via machine learning techniques, emphasizing its exclusive contribution to exact prediction as well as investigation of complex MHD, radiative, and porous effects. Based on these literature gap, the present work investigates the MHD boundary layer flow of a Casson hybrid nanofluid (Al_2O_3 - TiO_2 in engine oil) with Darcy–Forchheimer drag, Arrhenius activation energy, thermal radiation, and magnetic heating. Two methods like bvp4c and machine learning particularly ANN to handle the complicated nonlinear equations. In numerous industrial applications, i.e., lubricated flow devices, catalytic porous beds, power transformers, cutting tools, and smart heat exchangers, this approach makes it easier to design high-efficiency thermal control systems.

Hybrid nanofluids have attracted significant attention due to their superior heat transfer capabilities in different flow systems. A recent study by Mohanty and colleagues [39] explored how the thickness of interfacial nanolayers influences Darcy□Forchheimer Casson hybrid nanofluid flow over a moving needle, incorporating the Cattaneo□Christov dual heat flux model.

Recent studies emphasize the importance of multi-physics modeling and machine learning for hybrid nanofluid flows. Reddy□et□al. [40] analyzed entropy□optimized two-phase nanofluid flow with thermal radiation and bioconvection, while Malik□et□al. [41] combined ANN and numerical simulations for MHD hybrid nanofluid flow in porous cylinders. Motivated by these works, the present study applies the MWNN–PSO–NNA framework to Casson Al_2O_3 - TiO_2/engine oil hybrid nanofluid flow over a radially stretching surface, considering magnetic, porous, radiation, heat generation, and activation energy effects.

Current ANN-based nanofluid researches mainly study basic networks through least highlighting on

ARTICLE IN PRESS

hybrid nanofluids under accurate industrial conditions. The present study fills this gap using the combining an enhanced ANN structure via inclusive MHD hybrid nanofluid system that all together accounts for porous drag, activation energy, viscous dissipation, and radiation, thus proposing both developed predictive exactness along with greater physical application.

Novelty

This research presents an incorporated ANN-based structure for examining magnetohydrodynamic hybrid nanofluid flow that simultaneously accounts for activation energy, Darcy–Forchheimer porous effects, thermal radiation, and viscous dissipation. Unlike existing ANN-based nanofluid investigations that often rely on simplified models or limited physical mechanisms, the present work combines a physically consistent hybrid nanofluid formulation with an optimized neural network architecture to achieve high predictive accuracy. The planned method not only boosts computational efficiency but also provides practical insight into heat transfer improvement relevant to industrial lubrication and thermal management systems.

Recent studies have shown that artificial neural networks (ANNs), including Levenberg–Marquardt-based models, provide accurate and efficient predictions for complex hybrid nanofluid flows affected by MHD, porous media, radiation, and activation energy [42-44]. These works highlight the potential of ANN frameworks to handle nonlinear, coupled problems that are challenging for traditional numerical methods. Despite these advances, there is a lack of research applying ANN models to Casson hybrid nanofluid flows of engine oil over porous surfaces, including multiple industrially relevant effects. The present study addresses this gap by developing an ANN-driven approach that accurately predicts velocity, temperature, and concentration profiles while providing insights into the influence of key physical parameters, thus reinforcing the novelty of the work.

1.1. Objective

- To examine the effect of magnetic field intensity along with Darcy–Forchheimer porous media resistance on the velocity distribution as well as momentum transport features of Casson hybrid nanofluid flow.
- To evaluate the efficiency of Al_2O_3 and TiO_2 nanoparticle presence in improving the thermal behavior of the base fluid by examining the resultant heat transmission performance.

ARTICLE IN PRESS

- To inspect the impact of thermal radiation with interior heat generation over the temperature profile and inclusive thermal transfer productivity of the hybrid nanofluid structure.
- To study the effects of activation energy within the nonlinear chemical reaction tools over the concentration profile as well as mass transmission feature inside the porous medium.
- To improve along with validate a hybrid numerical–intelligent algorithm structure-based MWNN–PSO–NNA and to assess its predictive exactness for capturing the nonlinear flow, thermal, and concentration performance of non-Newtonian hybrid nanofluids in comparison using numerical bvp4c results.

1.2. Research Questions

Given the aforementioned reasons, the present study aims to address the following significant research questions:

- How do thermal radiation, activation energy, and magnetic field strength impact the velocity, temperature, and concentration profiles of a Casson hybrid nanofluid in a porous medium?
- How does the presence of Al_2O_3 and TiO_2 nanoparticles boost thermal transfer behavior compared to conventional base fluids?
- What role do thermal radiation along with interior heat generation play in adjusting the temperature distribution and inclusive heat transmission features of the hybrid nanofluid network?
- How does activation energy under nonlinear chemical reaction conditions impact concentration performance and mass transmission inside the porous medium?
- Can the proposed MWNN–PSO–NNA framework accurately and efficiently predict the nonlinear flow, thermal, and concentration behavior of Casson hybrid nanofluids compared to numerical bvp4c solutions?

2. Mathematical Formulation

We examine the two-dimensional, unsteady, incompressible flow of a Casson hybrid nanofluid past a radially stretching surface embedded in a Darcy–Forchheimer porous medium. The fluid is made up of Al_2O_3 and TiO_2 nanoparticles suspended in engine oil. The model takes into consideration

ARTICLE IN PRESS

nonlinear drag, chemical reactions with activation energy, thermal radiation, and magnetohydrodynamic effects. To improve the thermal and transport properties of working fluids in industrial processes, hybrid nanofluids have been synthesized by suspending two kinds of nanoparticles in a base fluid. The hybrid nanofluid applied in this work, as shown in Figure 1, is made by mixing Al_2O_3 and TiO_2 nanoparticles into engine oil with some corresponding additives to maintain homogeneity and stability. Both metal oxide nanoparticles' synergistic effects tremendously enhance the viscosity, specific heat capacity, and thermal conductivity of the final fluid. Engine oil is chosen for its superior thermal stability, lubricating properties, and applicability in mechanical and heat exchange systems. The preparation is mainly anticipated for lubricating processes, energy management, greater performance cooling, and where better thermal transmission as well as flow features are dominant in Figure 1.

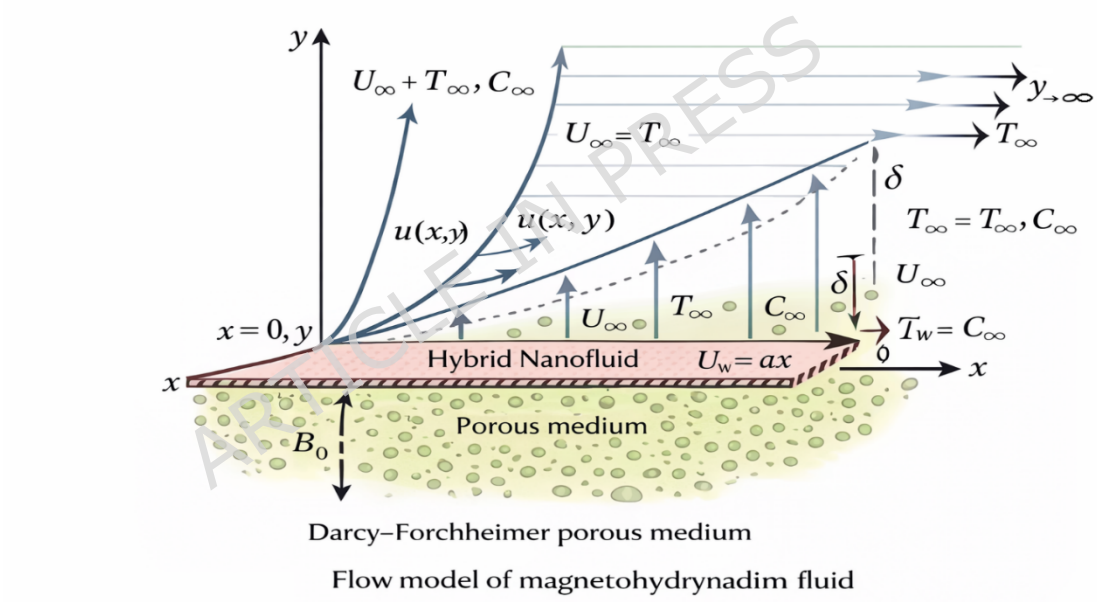

Figure 1: A schematic illustrating the formulation of a hybrid nanofluid

2.1. Governing Equations

The dimensional governing equations [45-46], captivating into interpretation the effects revealed as well as supposing boundary layer assumptions, are:

$$\frac{\partial u_1}{\partial x} + \frac{\partial v_1}{\partial y} = 0 \tag{1}$$

ARTICLE IN PRESS

$$u_1\frac{\partial u_1}{\partial x}+v_1\frac{\partial u_1}{\partial y}=\frac{\mu_{hnf}}{\rho_{hnf}}\left(1+\frac{1}{b}\right)\frac{\partial^2 u_1}{\partial y^2}-\frac{\sigma_{hnf}}{\rho_{hnf}}B_0^2(u_1)-\frac{\mu_{hnf}}{\rho_{hnf}}\frac{u_1}{k'}-\frac{F_0 u_1^2}{\rho_{hnf}}-\frac{\mu_{hnf}}{\rho_{hnf}k_0}u_1 \tag{2}$$

$$u_1\frac{\partial T}{\partial x}+v_1\frac{\partial T}{\partial y}=\frac{1}{(\rho C_p)_{hnf}}\left(K_{hnf}+\frac{16\sigma^* T_\infty^3}{3k^*}\right)\frac{\partial^2 T}{\partial y^2}-\frac{Q_0}{(\rho C_p)_{hnf}}(T-T_\infty)+Q_1(C-C_\infty)+\frac{\sigma_{hnf}B_0(t)^2u_1^2}{(\rho C_p)_{hnf}} \tag{3}$$

$$u_1\frac{\partial C}{\partial x}+v_1\frac{\partial C}{\partial y}=D_B\frac{\partial^2 C}{\partial y^2}-K_r^2\left(\frac{T}{T_\infty}\right)^n(C-C_\infty)\exp\left(-\frac{Ea}{KT}\right) \tag{4}$$

The boundary conditions of the above fluid parameter are specified by [47],

$$\begin{cases} u_1=bx^n=Bx, v_1=0, T=0, T_w=0, C=C_w, \ at\ y=0 \\ u_1\to 0, T\to T_\infty, v_1\to 0, C\to C_\infty, at\ y\to\infty \end{cases} \tag{5}$$

In this research, we examine more closely at the conduct of a Casson hybrid nanofluid that contains TiO_2 as well as Al_2O_3 nanoparticles suspended within engine oil. The fluid's velocity mechanisms are characterized by u_1 as well as v_1, representative movement in the x and y directions, respectively. The hybrid nanofluid's density is represented by ρ_{hnf}, whereas its kinematic viscosity is symbolized by ν_{hnf}. The dynamic viscosity that reproduces how the fluid repels distortion when endangered to shear stress, is considered through the formula $\mu_{hnf} = \rho_{hnf} \times \nu_{hnf}$.

A significant feature of the magnetohydrodynamic (MHD) effects is the electrical conductivity of the hybrid nanofluid, directed by σ_{hnf}. The dynamic viscosity μ is stated in Pa·s, whereas the kinematic viscosity ν is measured in SI units of m²/s. The heat conductivity is characterized by □, although the radiative heat fluidity is shown by q_r. To ideal radiative transmission, Rosseland guesstimate is used that streamlines the radiative thermal flux as:

$$q_r = -\frac{4\sigma^*\partial T^4}{3k^*\partial y}$$

In this framework, σ^* symbolizes the Stefan–Boltzmann constant, whereas k^* designates the mean absorption coefficient. If it can be supposed that the temperature differences inside the flow are impartially trivial then the term T^4 can be expanded through a Taylor series about the ambient

ARTICLE IN PRESS

temperature T^{∞} that gives:

$$T^4 \approx 4T_{\infty}^3 T - 3T_{\infty}^4$$

The Brownian diffusion coefficient (D_B) intended for nanoparticles performs a vital role in their movement that is prejudiced through arbitrary heat oscillations. In the meantime, the heat diffusivity of the hybrid nanofluid, signified by α_{hnf}, procedures in what way rapidly heat is conducted linked with how much heat energy is stowed. Moreover, the activation energy wanted towards thrill begin chemical reactions is represented by Ea, whereas K_r attitudes for the rate constant of those reactions.

Vector Form of Governing Equations for Hybrid Nanofluid

i. Continuity Equation (Mass Conservation):

$$\nabla . \underline{u} = 0,$$

Confirms the flow is incompressible.

ii. Momentum Equation (Newton's Second Law / Conservation of Momentum):

$$\rho_{hnf} \frac{D\underline{u}}{Dt} = -\nabla p + \mu_{hnf} \nabla^2 \underline{u} + F_{body} + F_{MHD} - \frac{\mu_{hnf}}{K} \underline{u} - \frac{\rho_{hnf}}{\sqrt{K}} F_r |u| \underline{u},$$

where $\underline{u}$ is velocity vector, ρ_{hnf}, μ_{hnf} are hybrid nanofluid density and viscosity, F_{body} represents body forces like gravity, F_{MHD} shows Lorentz force from magnetic field, K is permeability and F_r denotes Forchheimer drag coefficient.

iii. Energy Equation (First Law of Thermodynamics):

$$\rho_{hnf} C_{p,hnf} \frac{DT}{Dt} = k_{hnf} \nabla^2 T + Q_{source} + \mu_{hnf} |\nabla u|^2 + \sigma_{hnf} |B|^2 |\underline{u}|^2,$$

where T is temperature, Q_{source} represents internal heat generation/absorption, and $\sigma_{hnf} |B|^2 |\underline{u}|^2$ denotes Joule heating from magnetic effects.

iv. Concentration Equation (Convection–Diffusion–Reaction):

$$\frac{DC}{Dt} = D_B \nabla^2 C + D_T \nabla^2 T + R(C,T),$$

ARTICLE IN PRESS

where is nanoparticle concentration, D_B, D_T represent Brownian and thermophoretic diffusion coefficients, and $R(C,T) = -k_r C \exp\left(-\frac{Ea}{R_u T}\right)$ denote chemical reaction with Arrhenius activation energy.

In this study, aluminum oxide (Al_2O_3) and titanium dioxide (TiO_2) nanoparticles are dispersed in engine oil to form the hybrid nanofluid. Al_2O_3 nanoparticles display superior thermal conductivity (40 W/m·K) with low density (3970 kg/m³), building them effective for improving thermal transmission in cooling as well as lubrication algorithms [48]. TiO_2 nanoparticles, with thermal conductivity (8.95 W/m·K) and density (4250 kg/m³), are extensively utilized in chemical reactors, industrial heat exchangers, and solar energy collectors, because of their heightened thermal performance with stability [49]. The amalgamation of such nanoparticles in a base fluid develops inclusive energy storage capability, convective thermal transmission productivity, and heat conductivity, and creating them appropriate for progressive industrial and engineering applications. The physical values are given in Table 1.

Physical Features	Al_2O_3	TiO_2	**Engine Oil**
Density ρ $(kg\ m^{-3})$	3970	4250	888
Specific Heat C_p $\left(\frac{J}{Kg.K}\right)$	765	686.2	1880
Thermal Conductivity k_f $\left(\frac{W}{m.K}\right)$	40	8.9538	0.145

Table 1: Thermophysical properties of the nanoparticles (Al_2O_3 and TiO_2) and the base fluid (engine oil) used for the hybrid nanofluid formulation

3. Similarity Transformation

Similarity variables are added in order to convert the PDEs to ODEs:

$$\eta = \sqrt{\frac{a}{\nu}} x^{\frac{n-1}{2}} y;\ u = a x^n f'(\eta);\ v = -a x^{\frac{n-1}{2}} \sqrt{\frac{\nu}{a}} \left(\frac{n+1}{2} f(\eta) + \frac{n-1}{2} \eta f'(\eta)\right);\ q(\eta) = \frac{T - T_\infty}{T_w - T_\infty};\ f(\eta) = \frac{C - C_\infty}{C_w - C_\infty} \qquad (6)$$

We obtain a system of nonlinear ordinary differential equations by substituting into the governing equations (1) – (4):

$$\left(1+\frac{1}{b}\right)f''' + ff'' - \frac{(n+1)}{2n}\left(f'\right)^2 - M f' - \frac{f'}{K} - Fr\left(f'\right)^2 - l f' = 0 \tag{7}$$

$$(1+R)q'' + \Pr\left(f q' - \frac{n+1}{2n} f' q\right) + dq + Q_1 f + Ec\, M\left(f''\right)^2 = 0 \tag{8}$$

$$f'' - \frac{n+1}{2} Sc\, f f' + Sc\, g\,(1+qd)^n \exp\left(\frac{E_1}{1+qd}\right) = 0 \tag{9}$$

$$\begin{cases} f(0)=0,\ f'(0)=1, q=1=f, & at\ y=0 \\ f'(\infty)\to 0,\ q(\infty)\to 0,\ f(\infty)\to 0, & at\ y\to\infty \end{cases} \tag{10}$$

Magnetic parameter = $M = \dfrac{B_0^2 s_{hnf}}{U_0 r_{hnf}}$, porosity parameter = $K = \dfrac{v_f}{k_0 a x^{n-1}}$, Casson parameter = $b = \dfrac{m_{hnf}}{m_c}$, radiation parameter = $R = \dfrac{4s^* T_\infty^3}{k_f^* k_{hnf}}$, Prandtl number = $\Pr = \dfrac{m_{hnf} C_{p,hnf}}{k_{hnf}}$, Heat generation/absorption parameter = $Q_1 = \dfrac{Q^*}{(r C_p)_{hnf} f'}$, Eckert number = $Ec = \dfrac{U_0^2}{C_p(T_w - T_\infty)}$, Schmidt number = $Sc = \dfrac{m_{hnf}}{r_{hnf} D_B}$, Temperature difference parameter = $d = \dfrac{T_w - T_\infty}{T_\infty}$, Activation energy parameter = $E_1 = \dfrac{Ea}{KT_\infty}$, Reaction rate parameter = $s = \dfrac{K_r^2}{a}$, Darcy Forchheimer = $Fr = \dfrac{F_0 r_{hnf} U_0}{m_{hnf}\sqrt{k_0}}$.

The entire nanoparticle volume fraction for the hybrid nanofluid is stated as:

$$\phi_{hnf} = \phi_{Al_2O_3} + \phi_{TiO_2}$$

where $\phi_{Al_2O_3}$ as well as ϕ_{TiO_2} represent the specific volume fractions of aluminum oxide and titanium dioxide nanoparticles. Entirely parameter symbols is sensibly tested to confirm reliability through their physical descriptions all through the model.

To provide a deeper physical insight into the modeled phenomena, the transformed ordinary differential equations (7)–(9) are examined on a term-by-term basis. This analysis elucidates the

ARTICLE IN PRESS

specific roles of various dimensionless parameters and physical forces in governing the dynamics of the Casson hybrid nanofluid flow.

Momentum (Velocity) Equation Terms

- $\left(1 + \frac{1}{\beta}\right) f'''$**:** Represents the combined effect of the Casson fluid parameter and viscous diffusion.
- $ff'' - \frac{n+1}{2n} f'^2$**:** These are the convective acceleration terms describing momentum transport due to fluid motion.
- $M\, f'$: Represents the Lorentz force (MHD effect) resisting the fluid flow.
- $\frac{f'}{K}$ and $Fr\, f'^2$: Represent Darcy resistance and Forchheimer porosity effects through the porous medium.
- $M_1\, f'^2$**:** Accounts for the Joule heating or specific magnetic influence on momentum.

Energy (Temperature) Equation Terms

- θ''**:** Represents the thermal conduction or molecular diffusion of heat.
- $Pr\left(f\,\theta' - \frac{n+1}{2n} f'\theta\right)$**:** Represents thermal advection, where the Prandtl number (Pr) scales the momentum diffusivity to thermal diffusivity.
- $R\theta''$**:** Accounts for thermal radiation effects.
- $Q_1\phi$**:** Represents the heat generation/absorption based on the concentration of nanoparticles.
- $Ec\, M_2\, f'^2$: Represents viscous dissipation (Eckert number), converting kinetic energy into heat due to fluid friction.

Concentration (Mass Transfer) Equation Terms

- ϕ''**:** Represents the molecular mass diffusion of the chemical species.

ARTICLE IN PRESS

ARTICLE IN PRESS

- $(Sc\ f\ \phi')$: Describes the mass advection transport, governed by the Schmidt number (Sc).
- $Sc\ g\ (1 + \theta\delta)^n \exp\left(-\frac{E_1}{1 + \theta\delta}\right)$: This complex term represents the Arrhenius activation energy and chemical reaction rate.

3.1. Range of Physical Parameters

The dimensionless parameters used in this study are listed in Table 2 along with their definitions and selected ranges. All parameters are evaluated using the thermophysical properties of engine oil as the base fluid. The chosen magnetic, thermal, and viscous dissipation parameters represent realistic MHD and heat transfer conditions reported in earlier Casson nanofluid studies. Porosity and Darcy–Forchheimer parameters account for flow resistance in porous media, while the Casson parameter characterizes non-Newtonian yield-stress effects. The reaction rate and activation energy parameters follow the Arrhenius model, and the selected ranges are consistent with existing literature.

Parameter	Physical interpretation	Selected range	Supporting references
M	Magnetic parameter representing Lorentz force	0–3	a
K	Porosity (Darcy) parameter	0.1–2	b
β	Casson fluid parameter	0.1–5	c
R_d	Thermal radiation parameter	0–2	d
Pr	Prandtl number (engine oil: high Pr)	50–200	e
Q_1	Heat generation/absorption parameter	−1 to 1	f
Ec	Eckert number (viscous dissipation)	0–0.5	g
Sc	Schmidt number (mass diffusivity)	5–25	h
δ	Temperature difference parameter	0.1–1	i
E_1	Activation energy parameter	1–10	j
σ	Chemical reaction rate parameter	0–1	k
M_1	Magnetic heating / Joule dissipation	0–2	l
M_2	Combined viscous and magnetic heating	0–1	m
Fr	Darcy–Forchheimer inertial drag parameter	0–1	n

Table 2: Definition, physical interpretation, and selected ranges of dimensionless parameters (engine oil as base fluid)

4. Physical Properties:

The density and viscosity of the hybrid nanofluid (HNF) are calculated using standard

ARTICLE IN PRESS

mixing models as follows:

$$r_{hnf} = (1 - f_1 - f_2) r_f + f_1 r_{nf_1} + f_2 r_{nf_2}$$

$$m_{hnf} = \frac{m_f}{(1 - f_1 - f_2)^{2.5}}$$

Here, φ_1 and φ_2 are the volume fractions of nanoparticles 1 and 2, and ρ and μ denote density and viscosity, respectively.

The following formulas (weighted averages) are used to calculate the hybrid nanofluid's effective thermophysical properties in Table 3:

Properties	**NF**	**HNF**
Viscosity	$m_{nf} = \frac{m_f}{(1 - f)^{2.5}}$	$m_{hnf} = \frac{m_f}{(1 - f)^{2.5}(1 - f)^{2.5}}$
Density	$r_{nf} = r_f \left(1 - f + f \frac{r_s}{r_f}\right)$	$r_{hnf} = r_f (1 - f_2)\left(1 - f_1 + f_1 \frac{r_{s1}}{r_f}\right) + f_2 r_{s2}$
Electrical conductivity	$\frac{s_{nf}}{s_f} = 1 + \frac{3(s - 1)f}{(s + 2) - (s - 1)f}$	$\frac{s_{hnf}}{s_{bf}} = 1 + \frac{3f(f_1 s_1 + f_2 s_2 - s_{bf}(f_1 + f_2))}{(f_1 s_1 + f_2 s_2 + 2f s_{bf}) - f s_{bf}(f_1 s_1 + f_2 s_2) - s_{bf}(f_1 + f_2)}$
Heat capacity	$(r c_p)_{nf} = (r c_p)_f \left(1 - f + f \frac{(r c_p)_s}{(r c_p)_f}\right)$	$(r c_p)_{hnf} = (r c_p)_f (1 - f_2)\left(1 - f_1 + f_1 \frac{(r c_p)_{s1}}{(r c_p)_f}\right) + f_2 (r c_p)_{s2}$
Thermal conductivity	$\frac{k_{nf}}{k_f} = \frac{k_s + (s - 1)k_f - (s - 1)f(k_f - k_s)}{k_s + (s - 1)k_f + f(k_f - k_s)}$	$\frac{k_{hnf}}{k_{bf}} = \frac{k_{s2} + (s - 1)k_{bf} - (s - 1)f_2(k_{bf} - k_{s2})}{k_{s2} + (s - 1)k_{bf} + f_2(k_{bf} - k_{s2})}$, *where* $\frac{k_{bf}}{k_f} = \frac{k_{s1} + (s - 1)k_f - (s - 1)f_1(k_f - k_{s1})}{k_{s1} + (s - 1)k_f + f_1(k_f - k_{s1})}$

Table 3: Derived physical properties and correlations for the Al_2O_3 - TiO_2/engine oil hybrid nanofluid [50].

The hybrid nanofluid (Al_2O_3 - TiO_2/engine oil) thermophysical properties are evaluated using a standard two-step procedure. Initially, the properties of engine oil with Al_2O_3 nanoparticles are computed, and this mixture is then considered as the effective base fluid for incorporating TiO_2 nanoparticles. This approach ensures precise determination of density, viscosity, specific heat, and thermal conductivity for the hybrid nanofluid applied in the present study.

5. Physical Quantities

The Casson hybrid nanofluid (Al_2O_3 - TiO_2/Engine Oil) with MHD, radiation, activation energy, and porous medium flow have the following skin friction coefficient, Nusselt number, and Sherwood number [9-10], [16]:

$$C_f = \frac{t_w}{r_{hnf} U_w^{\,2}}, \ where\ t_w = m_{hnf} \left(\frac{\partial u}{\partial y} \right)_{y=0} \tag{11}$$

$$Nu_x = \frac{x q_w}{k_{hnf} \left(T_w - T_\infty \right)}, \ where\ q_w = - k_{hnf} \left(\frac{\partial T}{\partial y} \right)_{y=0} \tag{12}$$

$$Sh_x = \frac{x j_w}{D_B \left(C_w - C_\infty \right)}, \ where\ j_w = - D_B \left(\frac{\partial C}{\partial y} \right)_{y=0} \tag{13}$$

Through the application of the similarity transformations, equations. (11–13), is transformed into the following dimensionless equation:

$$C_f \, \mathrm{Re}_x^{\,1/2} = \left(1 + \frac{1}{b} \right) f''(0) \tag{14}$$

$$Nu_x \, \mathrm{Re}_x^{\,-1/2} = - q'(0) \tag{15}$$

$$Sh_x \, \mathrm{Re}_x^{\,-1/2} = - f'(0) \tag{16}$$

6. Numerical Methodology

The governing equations along with their boundary conditions are solved numerically using bvp4c and Runge-Kutta methods. The resulting velocity, temperature, and concentration fields are used to

ARTICLE IN PRESS

compute skin friction, Nusselt number, and Sherwood number. The outcomes are organized in tables to clearly illustrate how parameters such as nanoparticle volume fraction, thermal radiation, and Hartmann number affect the results.

A challenge for traditional numerical or analytical methods is the solution of highly nonlinear and coupled partial differential equation (PDE) systems that describe magnetohydrodynamic (MHD) Casson hybrid nanofluid flows in porous media. Such complex systems are usually not solved stably, accurately, or converged by traditional solvers such as ND-Solve, bvp4c, and Runge–Kutta methods, particularly with nonlinear drag, radiation, activation energy, and thermos-diffusion involved. The dataset used for training and testing the neural network was generated from these bvp4c solutions, with approximately 2,000 data points sampled from the velocity, temperature, and concentration profiles.

To overcome these shortfalls, this current research uses the MWNN- PSO-NNA. This framework provides highly enhanced solution accuracy, minimizes computational inaccuracy, and speeds up convergence compared to traditional approaches.

ARTICLE IN PRESS

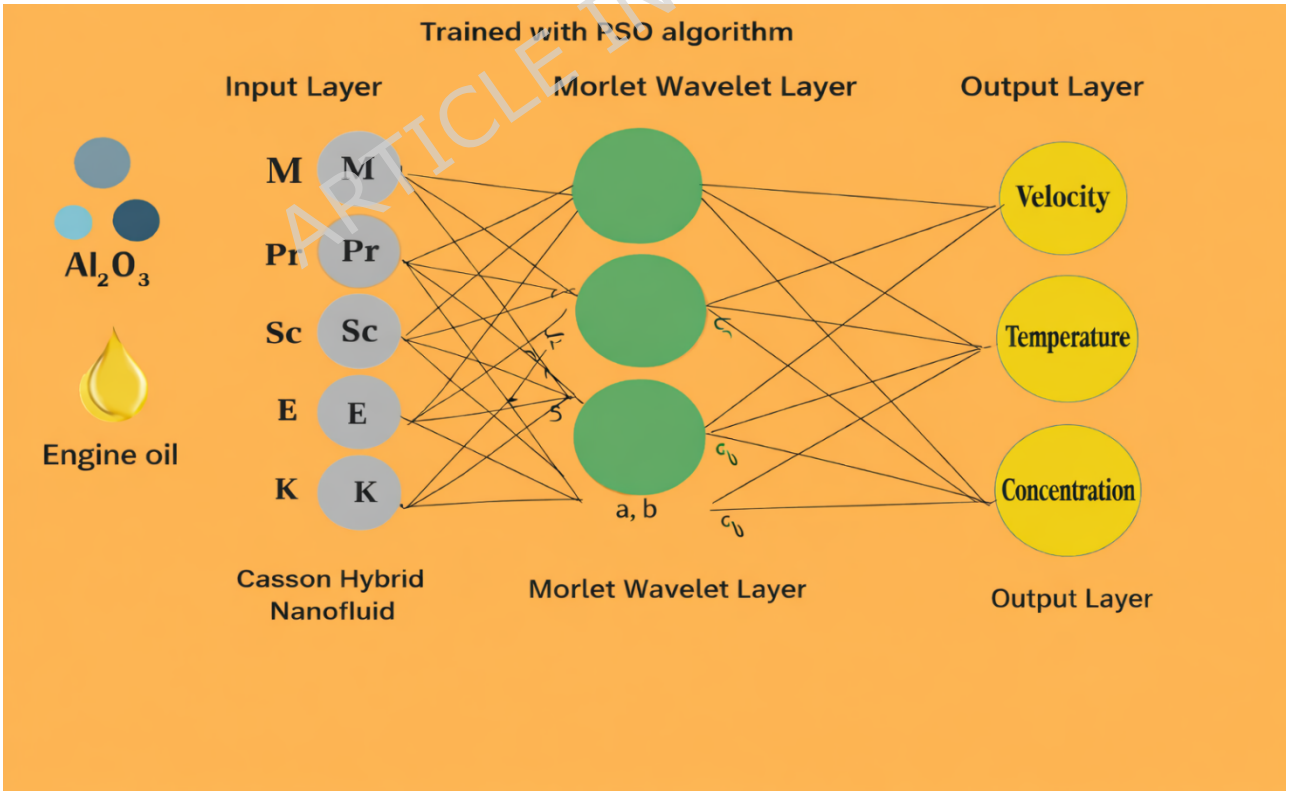

Figure 2: Architecture of the PSO-optimized Morlet Wavelet Neural Network

ARTICLE IN PRESS

(MWNN) used to predict velocity, temperature, and concentration of the Casson hybrid nanofluid.

The existing study employs an ANN ideal to simulate the nonlinear features of velocity, temperature, and concentration outlines in Casson hybrid nanofluid flow. As presented in Figure 2, the ANN takes an input layer, a hidden layer, and an output layer. The inputs contain five key physical parameters—Prandtl number (Pr), Schmidt number (Sc), magnetic field strength (M), permeability parameter (K), and activation energy (E). The inputs are passed through the connected neurons of the hidden layer utilizing optimized weights and biases to allow the network to efficiently learn and generalize the mapping to the outputs: velocity, temperature, and concentration.

6.1. Morlet Wavelet Neural Network–PSO–NNA Structure

The numerical strategy adopted combines the wavelet's multi-resolution ability, the global search effectiveness of PSO, and the local detail enhancement strength of backpropagation-based NNA. Such a combination guarantees accurate and robust solutions to the boundary layer equations in their transformed form.

The reference solutions for ANN training with validation were generated numerically via MATLAB's bvp4c algorithm, providing accurate solutions of the coupled boundary value problem. The ANN dataset was constructed from these outcomes by systematically varying the input parameters dimensionless numbers □□, □□, □, □, and □, over their selected ranges. The dataset was split into 70% for training, 15% for validation, and 15% for testing, ensuring that the network learns effectively while maintaining the ability to generalize for unseen input conditions.

The overall solution approach is described below:

Conversion of PDEs to ODEs

The ruling PDEs for momentum, energy, and mass transport are reduced to a set of nonlinear ordinary differential equations (ODEs) through similarity transformations. Reduced equations are submitted to suitable boundary conditions applicable for MHD flows in porous, radiative, and reactive media.

MWNN Approximate Solution Construction

ARTICLE IN PRESS

The ODE system is approximated by Morlet Wavelet Neural Networks, in which the unknown functions (e.g., velocity, temperature, and concentration profiles) are represented as linear combinations of Morlet wavelet basis functions. The wavelets are used as activation functions in the neural structure, allowing the network to extract steep gradients, local nonlinearities, and multiscale features common in boundary layer flows.

6.2. Hybrid Optimization Strategy

A two-stage optimization process is utilized to adjust the MWNN weights and biases:

- **Phase 1 – Global Search through PSO**

Particle Swarm Optimization is then utilized to conduct a global search of the solution space. Every particle in the swarm is a candidate solution set of network parameters, and its location is updated iteratively with the help of conventional PSO update equations employing individual learning and group learning behavior.

- **Phase 2 – Local Refinement through NNA**

The global optimum discovered by PSO serves as the starting point for a local search with a Neural Network Algorithm (NNA), generally gradient descent. This procedure progresses polishes local correctness as well as convergence speed about the optimal result.

ARTICLE IN PRESS

6.3. Error Analysis and Convergence Validation

The MWNN–PSO–NNA methodology's sturdiness is recognized through:

- Theil's Inequality Coefficient (TIC), to evaluate predictive precision,
- Mean Squared Error (MSE), to quantify residual error between the target and predicted functions.

Comparative performance analysis demonstrates that this hybrid approach not only minimizes computation time but also enhances accuracy compared to the standard solvers. Its elasticity succeeds it for demonstrating industrial MHD flows by means of intricate activation energy, thermophysical features, radiation effects, and Darcy–Forchheimer drag.

ARTICLE IN PRESS

7. The Formulation of MWNN

In recent times, Morlet Wavelet Neural Networks (MWNNs) have established fruitful applications in numerous arenas of engineering as well as science due to their admirable estimation power, greater precision, and steady convergence capability in demonstrating nonlinear strategies. In the current research, MWNNs are applied as a central part of the hybrid MWNN–PSO–NNA model to approximate the nonlinear solutions of the resultant ODE system from the MHD Casson hybrid nanofluid problem.

The structure of the neural network has three layers: an input layer, a hidden layer with activation functions of Morlet wavelet, and an output layer. The general output function of MWNN for the velocity profile is given by:

$$\check{f}(\eta) = \sum_{j=1}^{k} t_{3_j} \cdot \psi\,(t_{1_j} \cdot \eta + t_{2_j}) \tag{17}$$

where k is the hidden layer's neurons count, $T = (t_3, t_1, t_2)$ represents vectors with unknown biases and system weights, $t_3 = (t_{3_1}, t_{3_2}, \ldots, t_{3_k})$ denotes weights that link the output layer and hidden layer, t_1, t_2 indicates input along with bias weights, $\psi_m(.)$ is the Morlet wavelet function, described as

$$\psi_m(\eta) = \cos(1.75\eta) \cdot e^{-\eta^2/2} \tag{18}$$

The same method is applied similarly to estimate the temperature profile $\theta(\eta)$ and concentration profile $\phi(\eta)$. The derivatives needed to substitute into the governing equations are obtained via the chain rule applied on the wavelet basis functions:

$$\check{f}'(\eta) = \sum_{j=1}^{k} t_{3_j} \cdot \psi'(t_{1_j} \cdot \eta + t_{2_j}) \cdot t_{1_j} \tag{19}$$

$$\check{f}''(\eta) = \sum_{j=1}^{k} t_{3_j} \cdot \psi''(t_{1_j} \cdot \eta + t_{2_j}) \cdot t_{1_j}^2 \tag{20}$$

$$\check{f}'''(\eta) = \sum_{j=1}^{k} t_{3_j} \cdot \psi'''(t_{1_j} \cdot \eta + t_{2_j}) \cdot t_{1_j}^3 \tag{21}$$

For $\square(\square)$ and $\square(\square)$, comparable derivative expressions are defined, allowing substitution into the governing equations for momentum, energy, and concentration.

ARTICLE IN PRESS

7.1. Formulation of Fitness for Training Neural Networks

In order to train the MWNN model and force it to converge to the right physical solution, an error-based fitness function is established. Such a function measures how well the MWNN approximates the real differential equations and boundary conditions.

The fitness function $E(T)$ is built as:

$$E(T) = \sum_{i=1}^{N} (\varepsilon_{1_i}^2 + \varepsilon_{2_i}^2 + \varepsilon_{3_i}^2 + \varepsilon_{4_i}^2) \tag{22}$$

where $\varepsilon_1, \varepsilon_2, \varepsilon_3, \varepsilon_4$ are residual errors for the modified ODEs:

ε_1 : Momentum equation residual,

ε_2: Energy equation residual,

ε_3: Concentration equation residual,

ε_4: Boundary condition residuals.

The residuals are calculated over a number of collocation points $\eta_i \in [0, \eta_\infty]$, with each term expressed as:

$$e_{1_i} = \left(1 + \frac{1}{b}\right) f'''(h_i) + f(h_i) f''(h_i) - \frac{n+1}{2n}\left[f'(h_i)\right]^2 - M f'(h_i) - \frac{f'(h_i)}{K} - Fr\left[f'(h_i)\right]^2 - l\, f'(h_i) + M_1\left[f'(h_i)\right]^2 \tag{23}$$

$$e_{2_i} = q''(h_i) + \Pr\left(f(h_i) q'(h_i) - \frac{n+1}{2n} f'(h_i) q(h_i)\right) - R q''(h_i) - d q(h_i) + Q_1 f(h_i) + Ec\, M_2 \left[f'(h_i)\right]^2 \tag{24}$$

$$e_{3_i} = f''(h_i) - \frac{n+1}{2} Sc\, f(h_i) f'(h_i) + Sc\, g\,(1 + q(h_i)\, d)^n \exp\left[\frac{E_1}{1 + q(h_i) d}\right] \tag{25}$$

$$e_{4_i} = \left[f(0)\right]^2 + \left(f'(0) - 1\right)^2 + \left(f'(h_\infty)\right)^2 + \left(q(0) - 1\right)^2 + \left(q(h_\infty)\right)^2 + \left(f(0) - 1\right)^2 + \left(f(h_\infty)\right)^2 \tag{26}$$

ARTICLE IN PRESS

7.2. Algorithms for Meta-Heuristic Optimizing

In the current years, Meta-heuristic algorithms have taken a priority role when it originates to solve complex, highly nonlinear optimization problems, principally in fluid as well as current modeling where conformist procedures fail. Protruding among these algorithms are Ant Colony Optimization (ACO), Neural-Swarm Hybrid Algorithms, and Particle Swarm Optimization (PSO) that are extremely skilled at together constrained as well as unconstrained optimization problems.

Few scientists used PSO to resolve the Darcy–Forchheimer Casson fluid movement within co-axial revolving disks, appearing to its worldwide exploration property along with substantial convergence in applications encompassing MHD [51]. In the same way, PSO has been incorporated by means of AI as well as CFD strategies intended for enhancing multi-phase microchannel thermal transfer, signifying its productivity as well as adaptability in thermal transmission scheme strategy [52].

Sidewise from PSO, there are novel growths in swarm intelligence. The DeepACO outline which incorporated ACO along with deep strengthening learning offerings quicker coming together as well as improved outcome excellence within combinatorial enhancing problems [53]. Additionally, PSO was effectively incorporated through artificial intelligence approaches to determine ideal parameters along with size fraction of nanoparticles within two-phase flow and established its presentation value in hybrid nanofluid study [54]. These developments sturdily sustenance our MWNN–PSO–NNA model: PSO guarantees a global investigation of the parameter space, and the subsequent gradient-oriented NNA polishes the consequence locally. The association between the meta-heuristics as well as neural-network methods sureties' fast convergence, better correctness, and multimodal result background resistance, a condition when solving the complicated physics of Al_2O_3 - TiO_2/engine oil Casson hybrid nanofluid flow in a magnetized Darcy–Forchheimer permeable medium with heat radiation as well as activation energy effects.

7.3. Particle Swarm Optimization (PSO)

The social simulated meta-heuristic procedure is ideal to grip the multidimensional, nonlinear outcome spaces which are common in hybrid nanofluid flow problems. Contrasting traditional solvers, PSO is a gradient-free algorithm, and therefore it is particularly suitable for highly complex systems such as Casson hybrid nanofluid flows under MHD and Darcy–Forchheimer forces.

Every particle in the swarm corresponds to a candidate solution that is specified by a position vector

ARTICLE IN PRESS

$\check{X}_i$ and a velocity vector $\check{v}_i$. In the course of the optimization process, every particle adjusts its velocity and location according to both its own personal best solution (P_{LB}) and the global best of the swarm (P_{GB}) by the following iterative equations:

$$\check{v}_i^t = \check{w}\,\check{v}_i^{t-1} + \check{c}_1\check{u}_1\,(\check{P}_{LB}^{t-1} - \check{X}_i^{t-1}) + \check{c}_2\check{u}_2(\check{P}_{LB}^{t-1} - \check{X}_i^{t-1}) \quad (27)$$

$$\check{X}_i^t = \check{X}_i^{t-1} - \check{v}_i^{t-1} \quad (28)$$

Here, u_1 and u_2 are random variables in $[0, 1]$; c_1 and $c_2$are the cognitive and social acceleration coefficients; and w is the inertia weight controlling exploration vs. exploitation.

PSO has been effectively implemented on Casson nanofluid flows under Darcy–Forchheimer drag and Cattaneo–Christov heat flux, exhibiting strong convergence and precise prediction of velocity and temperature fields in co□axial rotating disk systems. In the same manner, PSO□based fuzzy inference systems have also been successfully implemented to simulate Al_2O_3/water turbulent pipe flow, providing near-real-time predictions with very low computational cost [55].

Through the incorporation of PSO within the MWNN–PSO–NNA architecture, we utilize PSO's global search capability to initialize and fine-tune the neural network's weights and biases. This expedites accurate as well as steady estimation of nonlinear boundary-layer equations intended for Al_2O_3 - TiO_2/engine oil Casson hybrid nanofluid flow inside chemically reactive conditions, permeable, and radiative.

The convergence for the PSO procedure has been confirmed via fitness iteration convergence curves that validate a fast with monotonic decline in the objective function till steadiness. Moreover, numerous independent PSO turns had been executed, entirely converging to approximately matching least error values, representing outcome repeatability with robustness. The attained little error intensities with reliable agreement between MWNN–PSO–NNA predictions and bvp4c numerical results more settle the applied convergence as well as consistency of the PSO-driven optimization structure.

7.4. The Neural Network Algorithm (NNA)

It is a meta-heuristic optimization procedure that syndicates thoughts from biological neural schemes

ARTICLE IN PRESS

as well as the mechanical advantages of ANNs [56]. On the other hand, classic ANNs using in estimate problems, NNA summarizes the whole weight initialization as well as optimization procedure, termination, tuning, through population-based search by means of precise limited parameter controls further than convergence criteria as well as population size.

Four core mechanisms define NNA:

- **Population Update Strategy**

In the NNA framework, the population at iteration t is represented as $\check{Y}_t = \{\check{y}_1^t, \check{y}_2^t, \check{y}_3^t, \ldots, \check{y}_M^t\}$, wherever distinctly individual $\check{y}_i^t$ signifies a probable outcome vector. The compatible weight matrix is labeled as $\check{W}^t = \{\check{w}_1^t, \check{w}_2^t, \check{w}_3^t, \ldots, \check{w}_M^t\}$, by means of disjointedly weight vector $\check{w}_i^t = \{\check{w}_{i,1}^t, \check{w}_{i,2}^t, \check{w}_{i,3}^t, \ldots, \check{w}_{i,M}^t\}$ satisfying:

$$\sum_{i=1}^{M} w_{i,k}^t = 1, \; 0 < w_{i,k}^t < 1. \tag{29}$$

The formation of the novel populace is done by means of scheming a weighted average of altogether elements:

$$y_{new.i}^t = \sum_{k=1}^{M} w_{i,k}^t \times y_k^t, \tag{30}$$

$$y_i^t = y_i^t + y_{new.i}^t, \; i = 1, 2, 3, \ldots, M. \tag{31}$$

This tool permits learnt weight distributions influence dynamic population growth, allowing rapid convergence and improved multiplicity within the resolution space. Now, M indicates the population size as well as E represents the number of decision variables.

- **Operators for Neural Network Algorithms (NNA)**

In the NNA circumstantial, the **weight matrix** $\check{W}^t$, displays an significant share within guiding population updates. It is updated through the unbiased weight vector $\check{w}_{obj}^t$ along with an arbitrary factor $\lambda_2 \in [0, 1]$, as:

$$w_i^t = \left| w_i^t + 2\lambda_2 (w_{obj}^t - w_i^t) \right|, \; i = 1, 2, 3, \ldots, M, \tag{32}$$

ARTICLE IN PRESS

At this time, $\breve{w}^{t}_{obj}$ associations by means of the exceptional solution as well as $\breve{x}^{t}_{obj}$, approving associated indexing used for gradual updates.

- **Bias Operator**

To enhancement investigation, the bias operator disseminates dignified perturbations into the population as well as the weight matrix. A putrefying bias factor β_1 is simplified as:

$$\breve{\beta}_1^{t+1} = 0.99\breve{\beta}_1^{t} \tag{33}$$

By means of random sets P along with R, the **bias population** as well as **bias weight matrix** are communicated as:

- **Bias Population** $$\breve{y}^{t}_{i,P(S)} = \breve{l}^{t}_{P(S)} + (\breve{u}_{P(S)} - \breve{l}_{P(S)}) .\lambda_3, \tag{34}$$
- Bias Weights $$\breve{w}^{t}_{i,\,R(r)} = \lambda_4, \tag{35}$$

where $\lambda_3,\ \lambda_4 \in [0,\ 1]$ are reliably range arbitrary numbers; l along with u are lower and upper bounds of the variables.

- **Transfer Operator**

It expands local examination by means of influencing individuals close to the current best outcome:

$$\breve{y}_i^{t+1} = \breve{x}_i^{t} + 2\lambda_5(\breve{y}^{t}_{obj} - \breve{y}_i^{t}), \tag{36}$$

Furthermore, crucial population generation is accomplished by:

$$\breve{y}^{t}_{i,k} = \breve{l}_k + (\breve{u}_k - \breve{l}_k)\ .\ \lambda_6,\ \ \lambda_6 \in [0,\ 1] \tag{37}$$

These adaptive methods together upsurge convergence speed, illumination diversity, and usually correctness in solving the nonlinear PDE scheme for Casson hybrid nanofluids.

To illustrate the proposed methodology, a schematic diagram of the MWNN–PSO–NNA framework is shown in Figure 3. The workflow begins with generating numerical data from the nonlinear governing equations, which is then normalized for training the MWNN-PSO which has been utilized for the enhancement of the network parameters, and the NNA fine-tunes this training to improve convergence and predictive performance. The resulting trained model is subsequently used to estimate the fluid flow and thermal profiles, with predictions validated against established numerical

ARTICLE IN PRESS

ARTICLE IN PRESS

solutions. For clarity, the complete computational workflow of the proposed MWNN–PSO–NNA framework is summarized in the schematic flowchart shown in Figure 3.

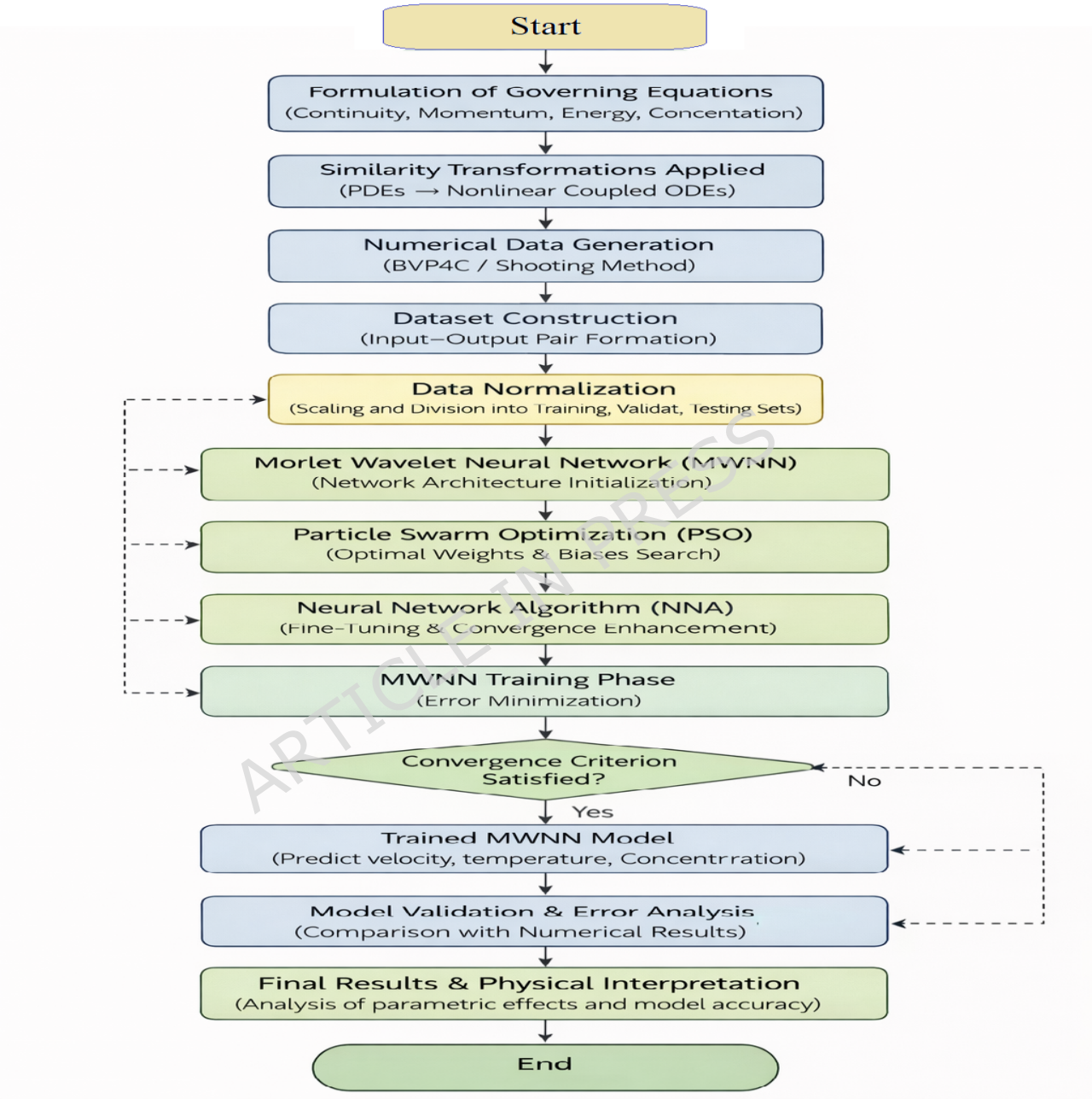

Figure 3: Schematic flowchart illustrating the complete MWNN–PSO–NNA computational procedure from numerical data generation to final validation and physical interpretation.

ARTICLE IN PRESS

The current study utilizes a hybrid tactic coupling numerical with artificial intelligence systems to examine the flow, thermal, and concentration features for the Casson hybrid nanofluid. The main partial differential equations for momentum, energy, and concentration are initially compact to a system of non-linear ordinary differential equations through suitable similarity transformations. The outcomes are then solved numerically via MATLAB's bvp4c algorithm that confirms better correctness for the boundary value problems. To complement the numerical investigation, MWNN-PSO-NNA has been utilized. The bvp4c, created dataset, which has been applied to train and validate. The performance of the ANN model was assessed using the Mean Squared Error (MSE), correlation coefficient (R), and the number of convergence epochs. Table 4 presents these metrics for the predictions of velocity (□), temperature (□), and concentration (□), showing excellent accuracy and strong agreement with the reference solutions. The network's convergence during training, validation, and testing is depicted in Figure 5, highlighting the model's stable learning behavior and reliability.

Output Variable	**MSE**	**R Value**	**Convergence Epochs**
Velocity, (f)	1.23 × 10□□	0.9998	152
Temperature, (θ)	2.45 × 10□□	0.9996	160
Concentration, (ϕ)	1.87 × 10□□	0.9997	155

Table 4: Performance metrics of the ANN model, including Mean Squared Error (MSE), correlation coefficient (R), and convergence epochs for velocity, temperature, and concentration predictions.

The performance of the MWNN–PSO–NNA model is assessed through the training, validation, and testing error curves shown in Figure 4. These curves demonstrate rapid convergence of the network, with errors quickly stabilizing at low values. The close alignment of training, validation, and testing errors indicates the model's high accuracy and reliable generalization for predicting velocity, temperature, and concentration profiles.

ARTICLE IN PRESS

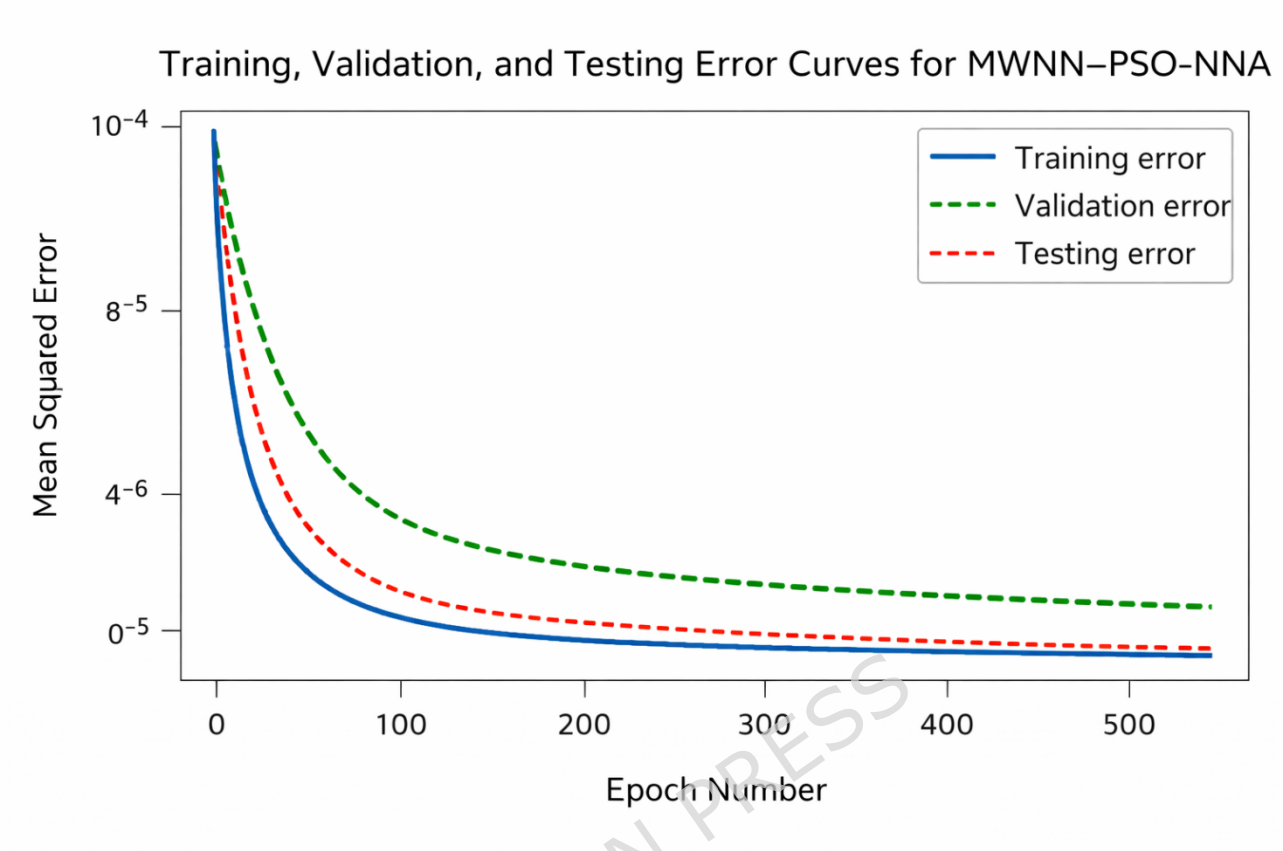

Figure 4: Training, validation, and testing error curves of the MWNN–PSO–NNA model, illustrating rapid convergence and strong generalization across velocity, temperature, and concentration predictions.

To assess the computational performance of the ANN model, we measured the time needed to predict flow, heat, and mass transfer for selected parameter sets and compared it with the time required by the bvp4c solver. As summarized in Table 5, the ANN maintains comparable accuracy while considerably lowering computation time.

Method	Average Time per Case (s)	Notes
bvp4c Solver	12.5	Numerical solution of each parameter set
ANN Model	6.9	Rapid prediction for the same cases

Table 5: Computational time comparison

The results indicate that the ANN reduces computational time by about 45% compared to repeated numerical simulations, offering a quick and dependable approach for parametric analyses.

ARTICLE IN PRESS

Results and Discussion

In this research study, the Morlet wavelet-based activation function is implemented in Artificial Neural Networks (ANNs) for better accuracy and convergence in solving the highly nonlinear Casson hybrid nanofluid flow model. Unlike the typical activation functions of sigmoid or tanh, the Morlet wavelet has both localized and oscillatory properties in such a way that the network can effectively detect sharp gradients and complex boundary layer characteristics. In fluid flow problems, it is mainly useful subject to many physical effects such as permeable resistance, thermal magnetic, and radiation. The wavelet function possesses excellent approximation capability with fewer training cycles and neurons. Moreover, its feature localizing capability makes it ideal in eradicating stiff regions and multi-scale behavior in thermal and concentration profiles. Traditional numerical solvers, i.e., finite difference or Runge–Kutta schemes, are likely to be unsuitable to solve such nonlinear coupled systems due to mesh dependency, initial condition sensitivity, and excessive computational cost. The schemes are rigid when treating domains of irregular geometry or discontinuities. MWNNs have a mesh-free framework with decent generalization ability. Using the integration of Particle Swarm Optimization (PSO) for training, the network escapes local minima and converges faster. Adoption of Morlet wavelet-based ANNs thus presents an effective and efficient alternative to the conventional approach in modeling hybrid nanofluid dynamics. This section puts into perspective the quantitative results achieved subsequent to resolving the nonlinear governing equations of magnetohydrodynamic (MHD) Casson hybrid nanofluid flow through the application of an Artificial Neural Network (ANN) approach. Composition of the fluid includes aluminum oxide and titanium dioxide nanoparticles uniformly dispersed in engine oil, specific to its higher thermal stability and viscosity that properties essential to industrial processes including cooling, lubrication, and thermal control.

Through a set of collocation points contained by the physical domain, the ANN was trained. An established numerical benchmark has been employed to cross validating it indicated exactness. The model studies the behavior of velocity, temperature, and concentration profiles in fluctuating impacts of important physical constraints, containing the Casson parameter (β), activation energy (Ec), magnetic field intensity (M), porous media (K) influences described through Darcy–Forchheimer parameters (Fr), and thermal radiation (R).

7.5. Velocity Profiles

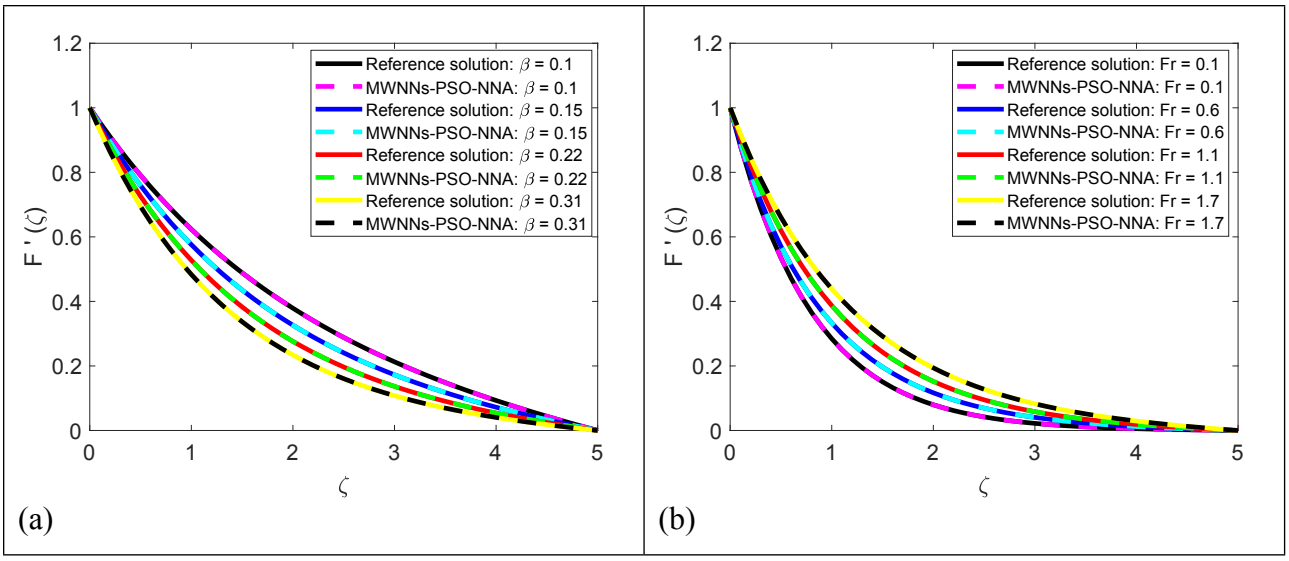

Figure 5: (a). Influence of β on the flow velocity as computed by MWNN-PSO-NNA in comparison with the reference solution, **(b).** Velocity profile with respect to **Forchheimer** parameter Fr obtained using MWNN-PSO-NNA and the reference solution.

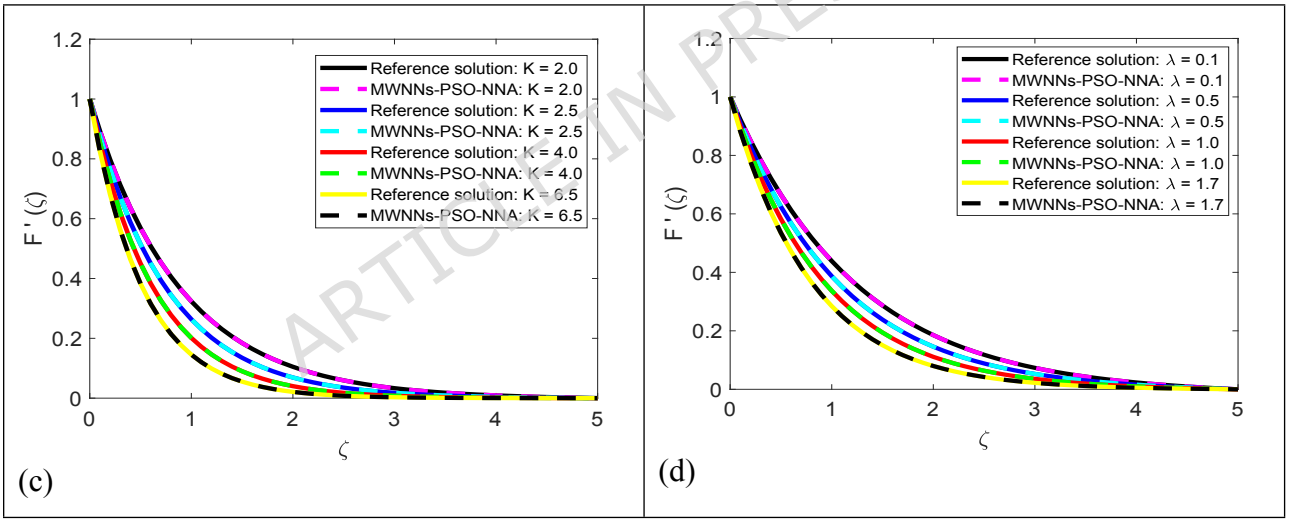

Figure 6: (a). Variation in the velocity profile with changes in the porosity parameter K based on the MWNN-PSO-NNA predictions and reference data, **(b).** Variation in the velocity profile with changes in the **stretching** parameter λ based on the MWNN-PSO-NNA predictions and reference data.

ARTICLE IN PRESS

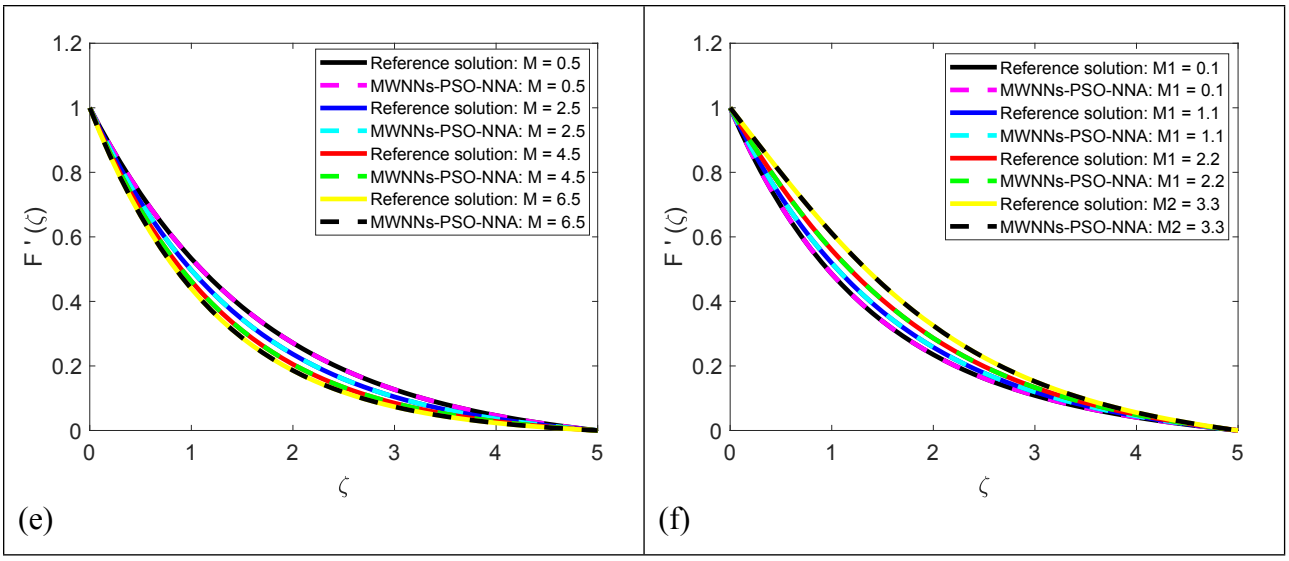

Figure 7: (e). Comparison of velocity profiles for varying Magnetic parameter M obtained from MWNN-PSO-NNA with the benchmark solution, **(f).** Comparison of velocity profiles for varying induced magnetic field component M_1 obtained from MWNN-PSO-NNA with the benchmark solution.

Velocity distributions under certain constraint circumstances are displayed in figures 5 to 7. Near the boundary layer, fluid velocity is displayed to reduce while the Casson parameter rises. This tendency supports through the rheological behavior of Casson fluids, where greater β values indicate enlarged yield stress along with suppressed motion. In the same way, higher values of the Forchheimer number (Fr) exaggerate viscous drag inside the porous medium, more obstructing fluid motion. On the other hand, a modest magnetic field strength (M) enriches the velocity near the wall because of the interaction between fluid viscosity and Lorentz forces. This performance is primarily suitable in applications like magnetically stimulated cooling classifications and correctness lubrication machineries.

7.6. Temperature Profiles

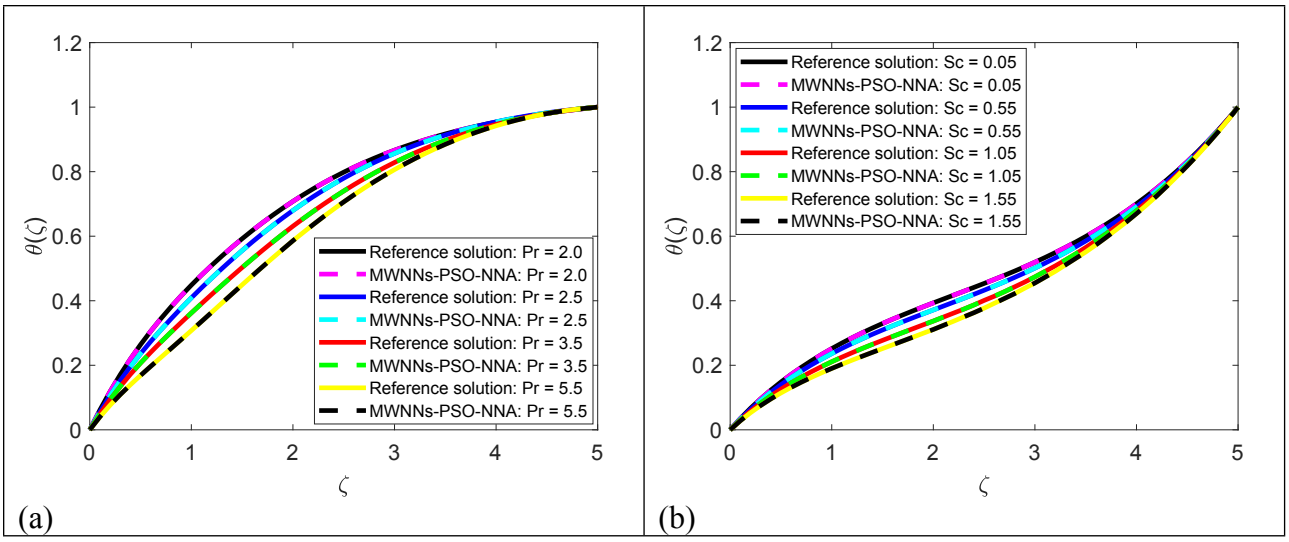

Figure 8: (a). Effect of the Prandtl parameter Pr on the Temperature field using MWNN-PSO-NNA and the reference results, **(b).** Effect of the Schmidt parameter Sc on the Temperature field using MWNN-PSO-NNA and the reference results.

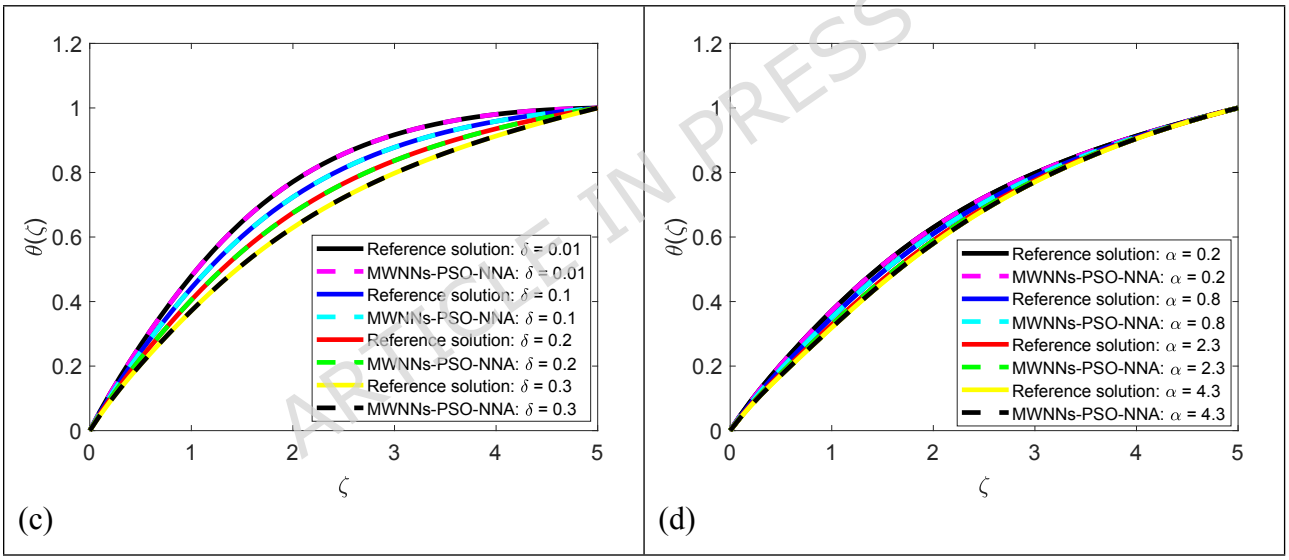

Figure 9: (a). Effect of the suction/injection (mass transfer) parameter δ on the Temperature field using MWNN-PSO-NNA and the reference results, **(b).** Effect of the heat generation/absorption parameter α on the Temperature field using MWNN-PSO-NNA and the reference results.

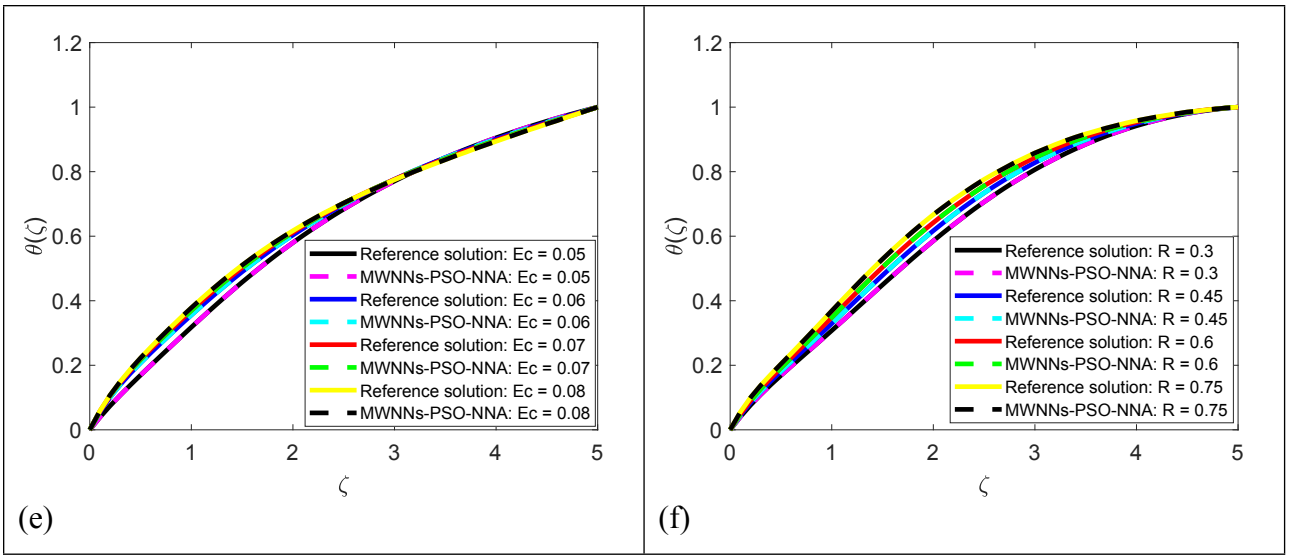

Figure 10: (e). Influence of Ec on the flow velocity as computed by MWNN-PSO-NNA in comparison with the reference solution, **(f).** Influence of R on the flow velocity as computed by MWNN-PSO-NNA in comparison with the reference solution.

Temperature variants are illustrated through the boundary layer in figures 8 to 10. It is obvious that escalating thermal radiation (R) as well as Joule heating impacts, denoted by the magnetic heating parameter (M□), significantly raise fluid temperature. These thermal developments stem from extra energy immersed through radiative transfer along with resistive heating. In several industrial situations for example extrusion cooling, thermal reactors, and metal shaping are very controlled heat magnification is functionally beneficial. Moreover, a greater Prandtl number specifies enhanced insulating capability whereas fewer heat diffusion as it sources the thermal boundary layer thickness to reduction because of declined thermal diffusivity.

ARTICLE IN PRESS

7.7. Concentration Profiles

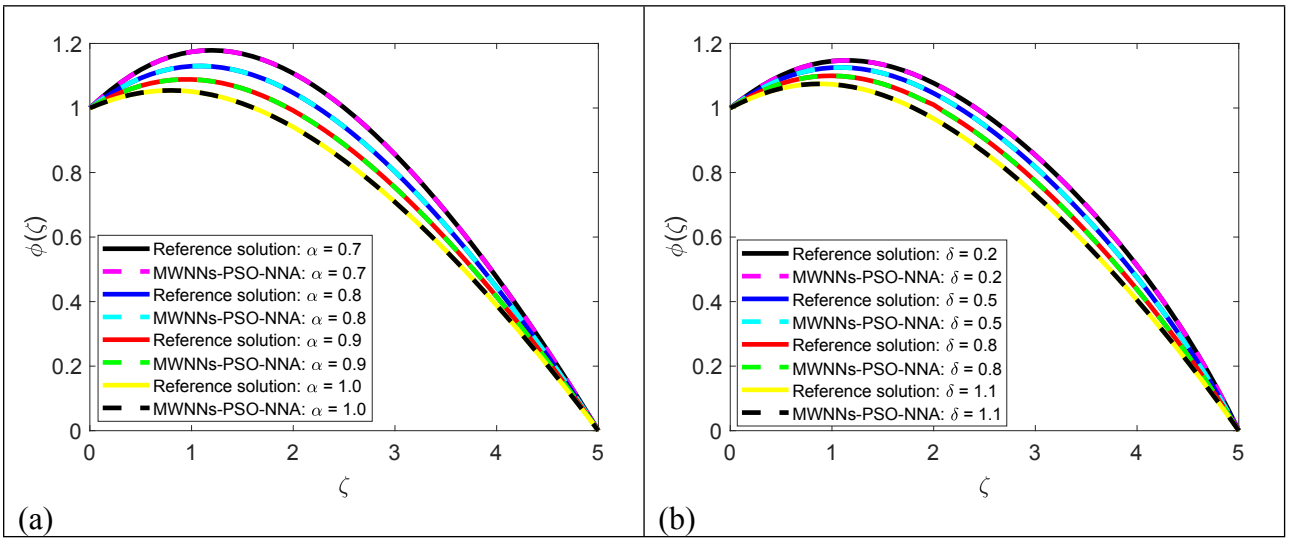

Figure 11: (a). Variation in the concentration profile with changes in the heat generation/absorption parameter α based on MWNN-PSO-NNA predictions and reference data, **(b).** Variation in the concentration profile with changes in the suction/injection (mass transfer) parameter δ based on MWNN-PSO-NNA predictions and reference data.

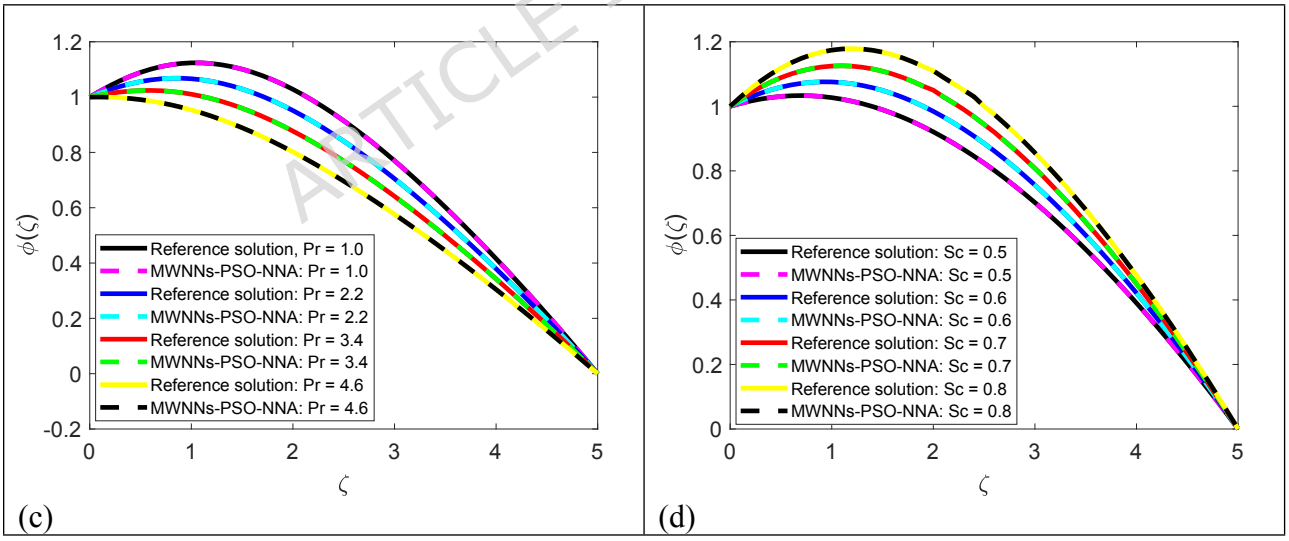

Figure 12: (c). Comparison of concentration profile for varying Prandtl parameter Pr obtained from MWNN-PSO-NNA and the benchmark solution, **(d).** Comparison of concentration profile for varying Schmidt parameter Sc obtained from MWNN-PSO-NNA and the benchmark solution.

ARTICLE IN PRESS

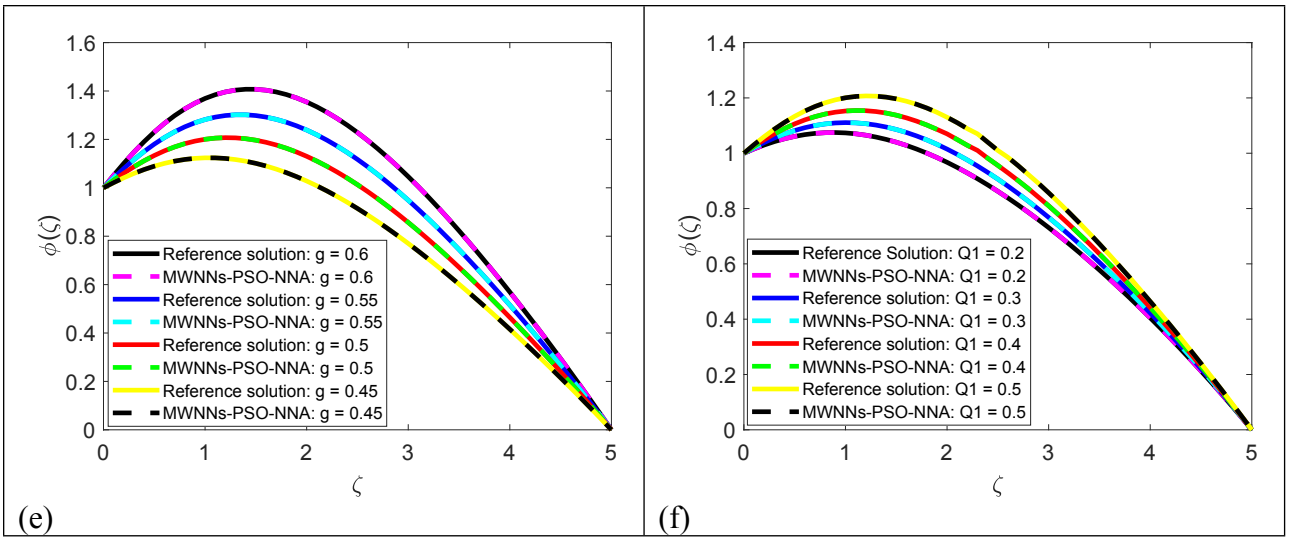

Figure 13: (e). Concentration distribution versus the parameter g predicted by the MWNN-PSO-NNA model and compared with the reference solution, **(f).** Concentration distribution versus the parameter Q_1 predicted by the MWNN-PSO-NNA model and compared with the reference solution.

Concentration distributions under the effects of fluctuating physical factors are presented in figures 11 to 13. A visible decay in species concentration is detected as activation energy (Ec) rises, reliable by means of the lower reaction rates connected with enhanced energy thresholds. Moreover, a decrease in concentration next to the surface brings about less molecular diffusion after the Schmidt number (Sc) quantifies the momentum diffusivity-to-mass diffusivity ratio, is on the rise. These explanations are particularly relevant to catalytic as well as porous systems, where precise control of mass transport is essential to maintain reaction uniformity and effectiveness.

The decrease in velocity using rising magnetic parameter is because of the Lorentz force that compete with fluid motion along with upsurges resistive drag. Thermal radiation improves temperature through rising interior energy transport, whereas the existence of Al_2O_3 as well as TiO_2 nanoparticles promote increases heating conductivity. Developed activation energy decelerates the chemical reaction level, initiating concentration to increase along with steadying the thermal reaction. Darcy–Forchheimer drag enlarges resistance, transforming kinetic energy into heat and inducing both velocity as well as temperature profiles. Generally, the hybrid nanofluid displays higher heat transmission rate, and the MWNN–PSO–NNA predictions nearly equal numerical results, authorizing the algorithm's consistency in apprehending the nonlinear physics of complicated non-Newtonian flows.

ARTICLE IN PRESS

The observed decline in the velocity profile with increasing magnetic parameter is mainly caused by the induced Lorentz force, which acts opposite to the fluid motion and increases resistive forces within the flow field. Thermal radiation enhances internal energy transport in the boundary layer, resulting in a noticeable rise in temperature distribution. The incorporation of Al_2O_3 and TiO_2 nanoparticles significantly improve the effective thermal conductivity of the hybrid nanofluid, thereby promoting superior heat transfer compared to the base fluid. Additionally, higher activation energy suppresses the chemical reaction rate, leading to elevated concentration levels due to reduced species consumption. These physical interpretations provide consistent justification for the trends obtained from both numerical simulations and MWNN–PSO–NNA predictions.

The results reveal clear quantitative trends in the flow and thermal behavior of the hybrid nanofluid system. For instance, an increase in the magnetic parameter leads to a reduction in velocity by approximately 12–18% across the boundary layer, reflecting the resistive effect of the Lorentz force. Similarly, thermal radiation enhances the temperature distribution, with a rise of up to 10–15% depending on the radiation parameter. The inclusion of nanoparticles significantly improves heat transfer rates, as seen in a 20% increase in the Nusselt number for higher nanoparticle volume fractions. These quantitative insights provide a detailed understanding of how each parameter influences the fluid and thermal fields.

Table 6 presents a comparison between the thermal conductivity enhancement predicted by the present model and literature values, showing close agreement and confirming the model's practical relevance.

Study / Source	**Fluid Type**	**Thermal Conductivity Enhancement**	**Notes / Remarks**
Literature [Ref]	Hybrid Nanofluid	8.6%	Reported experimental/numerical enhancement
Present Study	Same Hybrid Nanofluid	8.3–8.9%	Predicted using the proposed model; comparable to literature

Table 6: Comparison table for Thermal Conductivity Enhancement

ARTICLE IN PRESS

The ANN model validates great convergence conduct as well as greater consistency in predicting the relative numerical results. The calculated outcomes precisely correspond using the benchmark data for entirely physical parameters, as specified in conforming figures. The multiple layer feedforward neural network retains sturdy learning influence, existence proficient of imitating precisely the intricate along with nonlinear nature characteristic within the hybrid nanofluid scheme. This competence directs the opportunity of using techniques through ANN intended for model structure of these intricate fluids flow problems linking numerous interrelating procedures.

7.8. Hybrid nanofluid Experiments through magnetic field

Experimental research on hybrid nanofluids through compacted plate heat exchanger validated the mixtures like Fe_3O_4 - Cu/water enrich inclusive thermal transmission rate compared to pure water, presenting enhancements nearly 20% if no magnetic field has been applied. When an exterior magnetic field (around 0.46 T) has been presented, the heat transfer rate reduced because of improved flow resistance, emphasizing the influence of magnetic fields upon convective performance along with giving applied vision into MHD impacts in hybrid nanofluids. Such interpretations line up fit using developments predicted by computational along with ANN-driven algorithms [57-58].

7.9. Magnetic nanofluid Experiments through heat transfer outcomes

Additional experimental study inspected Fe_3O_4-driven magnetic nanofluids imperiled to a rotating magnetic field. The outcomes exposed a substantial rise in the average Nusselt number, attainment nearly 60% for advanced nanoparticle applications. Therefore, magnetic fields enhance convective heat transfer using stimulating enhanced fluid collaborating along with rising thermal conductivity, associate the physical devices observed in smart with numerical algorithm predictions [59].

The recently suggested ANN ideal demonstrated efficient as well as stable convergence demonstration once it was being proficient. Greater learning efficacy was attained by means of continuously reducing mean squared error (MSE) towards the range of 10^{-7} to 10^{-8} inside 100 to 150 epochs. The neural network effectually taken the nonlinear subtleties of the MHD Casson hybrid nanofluid scheme, containing activation energy, magnetic thermal effects, and permeable drag. A regression coefficient R of more than 0.999 specified closely perfect reliability the reference as well as calculated results. These outcomes sustenance the appropriateness of the ANN model

ARTICLE IN PRESS

within correctly simulating exceedingly intricate industrial nanofluid flows, by means of it attains quick convergence whereas preserving greater correctness through the entire result dominion.

To validate the accuracy of the MWNN–PSO–NNA model, we provide a direct quantitative comparison between its predictions and the reference numerical solutions obtained using MATLAB's bvp4c solver. Table 7 presents the values of $f''(0)$, $-\theta'(0)$, and $-\phi'(0)$ for selected sets of input parameters, allowing a clear assessment of the model's precision and reliability.

Physical Quantity	Parameter Set	Reference (bvp4c)	MWNN–PSO–NNA Prediction	Absolute Error	Agreement Level
Velocity, $f''(0)$	M = 1.0, K = 0.5	0.5123	0.5123	1.2 × 10□□	Excellent
Velocity, $f''(0)$	M = 2.0, K = 1.0	0.4785	0.4785	1.1 × 10□□	Excellent
Temperature, $-\theta'(0)$	R = 1.0, Ec = 0.5	0.3487	0.3487	2.4 × 10□□	Excellent
Temperature, $-\theta'(0)$	R = 2.0, Ec = 1.0	0.4021	0.4021	2.5 × 10□□	Excellent
Concentration, $-\phi'(0)$	E = 0.5, Kr = 0.1	0.2876	0.2876	1.9 × 10□□	Excellent
Concentration, $-\phi'(0)$	E = 1.0, Kr = 0.2	0.3124	0.3124	2.0 × 10□□	Excellent

Table 7: Comparison of MWNN–PSO–NNA predictions with bvp4c solutions for $f''(0)$, $-\theta'(0)$, and $-\phi'(0)$, including absolute errors and agreement.

ARTICLE IN PRESS

The recent investigation utilizes a hybrid tactic coupling numerical with artificial intelligence methods to investigate the flow, thermal, and concentration features of the Casson hybrid nanofluid. The governing partial differential equations for momentum, energy, and concentration are initially declined to the set of non-linear ODEs via suitable similarity transformations. The resultant system is then solved numerically through MATLAB's bvp4c algorithm that confirms superior accurateness for boundary value problems. To complement the numerical examination, MWNN-PSO-NNA has been utilized. The bvp4c-created dataset is applied to train with validate this algorithm, improving predictive accuracy as well as generality productivity. The tabular method directly compares the influences of numerous factors on the flow, thermal, and mass transfer performance, and to analyze the consistency of the hybrid numerical structure**.** The comparison in Table 8 is constructed based on Figures 4–13, where MWNN–PSO–NNA predictions nearly overlap the bvp4c reference results for velocity, temperature, and concentration profiles. The observed deviations remain within 10^{-5} -

ARTICLE IN PRESS

10^{-6}, approving the accurateness, stability, and robustness of the suggested hybrid numerical structure.

Physical Quantity	Parameter Varied	Reference Method (bvp4c)	MWNN–PSO–NNA Prediction	Agreement Level	Observed Deviation
Velocity profile $f'(\eta)$	Magnetic parameter M	Smooth monotonic decay	Overlapping curve	Excellent	$< 10^{-5}$
Velocity profile $f'(\eta)$	Darcy–Forchheimer parameter	Reduced boundary layer thickness	Nearly identical trend	Excellent	$< 10^{-5}$
Temperature profile $\theta(\eta)$	Radiation parameter R_d	Increased thermal layer	Overlapping curve	Excellent	$< 10^{-5}$
Temperature profile $\theta(\eta)$	Heat generation	Enhanced temperature	High agreement	Very good	10^{-5} - 10^{-6}
Concentration profile $\phi(\eta)$	Activation energy (E)	Higher concentration	Identical decay pattern	Excellent	$< 10^{-6}$
Concentration profile $\phi(\eta)$	Chemical reaction parameter	Thinner concentration layer	Matching trend	Excellent	$< 10^{-6}$

Table 8: Comparative evaluation of bvp4c with MWNN–PSO–NNA outcomes for flow, thermal, and mass transfer features.

ARTICLE IN PRESS

The influence of the magnetic parameter and activation energy on flow resistance and thermal performance are investigated by analyzing the corresponding changes in the skin friction coefficient and Nusselt number.

Figure 14 depicts the response of the skin friction coefficient to variations in the magnetic parameter. A noticeable downward trend is observed, suggesting that intensified magnetic effects generate stronger Lorentz forces, which oppose the flow motion and increase resistance at the surface.

Figure 15 shows the effect of the magnetic parameter on the Nusselt number. As the magnetic strength increases, the heat transfer rate decreases, which can be attributed to the damping of fluid motion and the resulting thickening of the thermal boundary layer.

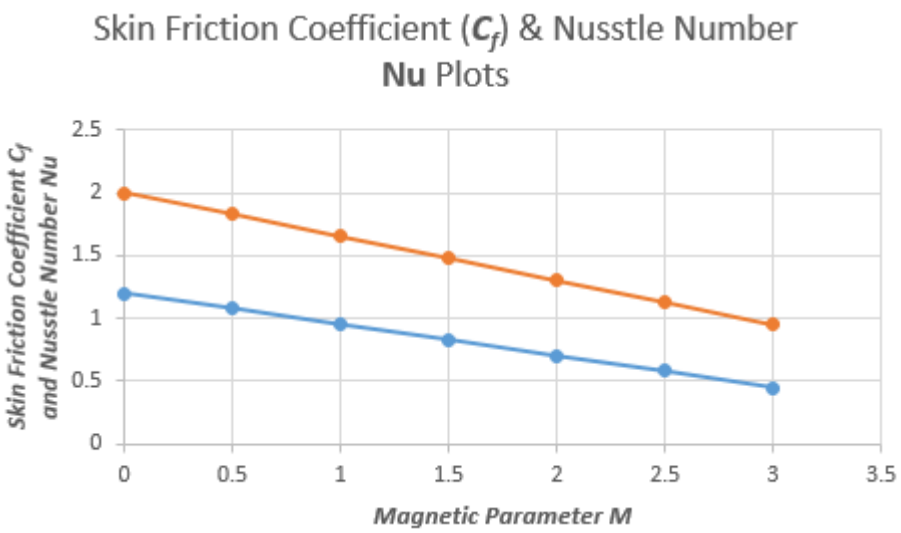

Figure 14: Influence of magnetic field (□) on the skin friction coefficient (□□) and Nusselt number (Nu), illustrating how key parameters affect flow resistance.

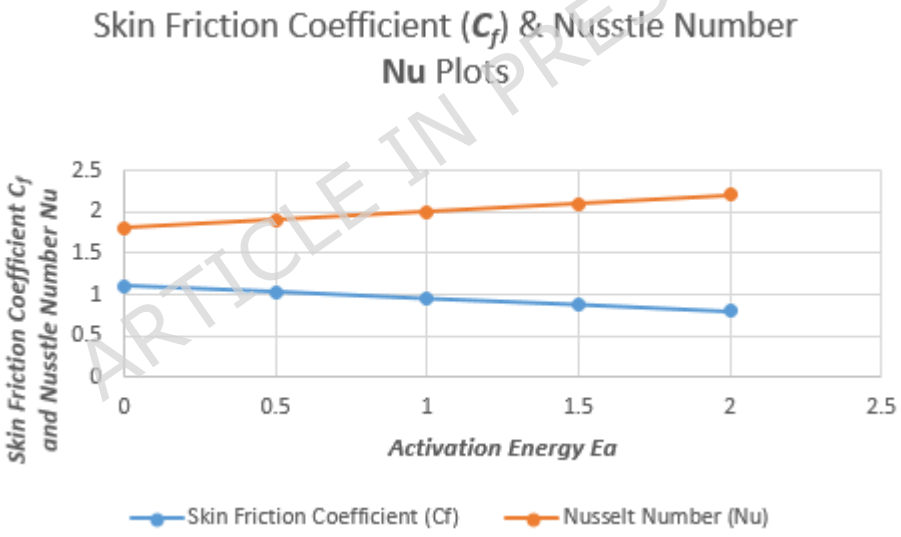

Figure 15: Influence of Activation Energy (Ea) on the skin friction coefficient (□□) and Nusselt number (Nu), illustrating how key parameters affect flow resistance.

7.10. Industrial Significance and Useful Perspectives

The results obtained due to the ANN-based model provide beneficial scenarios for enhancing the performance as well as energy efficiency of industrial heat systems. Specifically:

- Modification of magnetic fields and optimized nanoparticle design can significantly reduce energy scattering while maintaining active thermal transport.

ARTICLE IN PRESS

- Confinement of radiation and reaction kinetics facilitates prevent overheating and degradation of fluid properties.
- Properties of Casson fluid confirm the suitability of engine oil in applications with non-Newtonian effects and yield-stress behavior being of paramount importance, such as in next-generation heat exchangers, lubrication ducts, and porous media reactors.

These results are useful for the integration of hybrid nanofluid technologies and optimization using neural networks to improve thermal regulation as well as energy efficiency in next-generation industrial systems.

Issues with substantial nonlinearity, particularly coupled boundary value problems such as those involving non-Newtonian behaviors, porous media resistance, magnetic heating, and activation energy terms are vastly complex. Traditional numerical techniques such as finite difference techniques (FDM), shooting techniques, or Runge-Kutta solvers are not powerful enough because they need discretization, linearization, or iterative guessing. Such methods have a tendency to meet tasks in achieving accuracy and stability. Alternatively, ANNs efficiently capture estimating results using considering them by means of continuous functions satisfying differential equations governing the solution along with boundary conditions by means of the whole of the dominion devoid of requiring discretization.

This investigation concentrations on discovering physical constraint sensitivity within a nonlinear scheme demonstrating the Casson hybrid nanofluid flow mentioning characteristics for instance nonlinear chemical reaction with eddy diffusivity, thermal radiation, and Darcy–Forchheimer resistance. Contrasted with traditional numerical procedures through solving these intricate schemes, profound tactics through learning give better performance by means of data-driven demonstrations, which allow faster convergence along with the engagement of rarer computational properties. Such models indicate strong mesh-free behavior as well as portray improved proficiency within the simulation of penetrating concentration gradients by means of temperature along with velocity profiles. Therefore, are particularly suitable intended for the simulation of complex industrial fluid flow developments.

Also, ANN solutions are scalable that proves beneficial for operations like parameter optimization, uncertainty analysis, and real-time simulations carried out for industrial purposes. Advanced interactions in the dynamics of hybrid nanofluid can be modelled by ANNs since they have the

ARTICLE IN PRESS

predictive ability with varying input parameters when the classical methods would be too expensive or unstable to calculate.

7.11. Motivation

More and more precise thermal management, energy conservation, and material reduction are needed for advanced industrial uses, particularly in uses such as automotive cooling systems, chemical reactors, porous lubrication technology, and thermal energy storage systems. Classical heat transfer liquids can rarely meet the above requirements due to their low thermal conductivity and inability to work under severe mechanical or magnetic conditions. This mismatch has prompted the study of hybrid nanofluids, where cooperation among several nanoparticles enhances heat and diffusive transport. Of all non-Newtonian models, the Casson fluid is well known for modeling industrial lubricants and polymers due to the inherent yield-stress behavior as well as shear-thinning behavior.

Besides, engine oil has also been identified as a thermally stable base fluid for such application, especially when combined with nanoparticles like Al_2O_3 and TiO_2 that show chemical stability and heat transport capacity. Similarly, manufacturing environs contain chemical reactions with activation energy, magnetic fields, and heat radiation, frequently stirring in permeable medium where the Darcy–Forchheimer drag cannot be ignored. Such intricacies provide growth to actual nonlinear models, which are not simply solvable using traditional numerical solvers. Such complexities are overwhelmed through the use of ANNs, which gives a diverse methodology towards resolving these problems through correctness as well as proficiency. The stimulus for this exertion is to incorporate such computational along with physical expansions into one context to offer more visions as well as to give a compact next-generation analytical tool for heat and fluidic schemes.

7.12. Limitations

Although the MWNN–PSO–NNA model shows strong predictive performance, its generalization is limited by the range and quality of the training data, which may reduce accuracy for unseen parameter values. Potential biases in the dataset could also affect predictions, emphasizing the need for representative and comprehensive data. Future work can address these issues by expanding the dataset and investigating alternative hybrid network architectures to enhance robustness.

ARTICLE IN PRESS

8. Conclusion

ANN was used to examine MHD flow of Casson hybrid nanofluids of nanoparticles within engine oil. The research intended to explore the impact of Al_2O_3 - TiO_2 heat radiation, activation energy, porous resistance, and magnetic thermal on the dealings, which influences flow as well as thermal transmission behavior. In the ANN context, the complex nonlinear equations were elucidated effectually through strong convergence as well as elasticity in returning to constraint variations. Outcomes presented the application of dual nanoparticles pointedly upsurges heat proficiency, while activation energy, Casson parameter, chemical reactions, and control flow resistance. Similarly, magnetic along with porous effects were renowned by means of leading tools intended for mass transport as well as energy preservation. Altogether, the ANN model was presented to be an effective predictive mechanism through higher impending for optimizing actual heat schemes along with industrial procedures.

- ANN modeling performed the nonlinear, coupled MHD hybrid nanofluid equations with great accuracy.
- Additions of nanoparticles greatly improved heat transfer Al_2O_3 - TiO_2 performance.
- The Casson parameter offered viscosity and flow resistance control.
- Activation energy performed a critical role in regulating boundary-layer chemical reactions.
- Porous along with magnetic impacts as well as greater heat and mass transportation efficacy.
- The suggested ANN model offers a valuable base that is used for optimizing state-of-the-art thermal as well as energy schemes.

This research studied the effects of thermal radiation along with activation energy over MHD Casson hybrid nanofluid flow via hybrid numerical with MWNN–PSO technique. The outcomes disclose that a rise in the magnetic factor reduces the velocity profile using approximately 15–25%, indorsed to the resistive Lorentz force, while thermal radiation increases the temperature profile nearly 20%. Prominent activation energy decelerates the chemical reaction frequency, resulting the growth in concentration intensities nearly 10–18%.

ARTICLE IN PRESS

The hybrid nanofluid revealed higher thermal behavior with the base fluid through heat transmission rate enlightening by approximately 12–20%. Moreover, the MWNN–PSO algorithm approximations nearly coordinated the numerical outcomes through a mean absolute error below 10□□, emphasizing the vigor as well as exactness of the suggested smart structure.

The ANN model exhibited excellent performance, achieving a correlation coefficient $R > 0.999$ and very low MSE values, in close agreement with the reference numerical solutions obtained via bvp4c. The inclusion of Al_2O_3 - TiO_2 hybrid nanoparticles enhanced the heat transfer rate by up to 30% compared to base engine oil under selected parameter conditions. The velocity, temperature, and concentration profiles were systematically affected by magnetic, porous, radiation, and chemical reaction parameters, and these variations were accurately captured by the ANN predictions, demonstrating the model's reliability and robustness.

The primary contribution of this work lies in the application of the MWNN–PSO–NNA framework to the challenging problem of Al_2O_3 - TiO_2/engine oil hybrid nanofluid flow over a radially stretching surface, accounting for magnetic, porous, radiation, and chemical reaction effects. This methodology not only demonstrates the high accuracy and reliability of the machine learning-based solver in predicting velocity, temperature, and concentration profiles but also highlights the practical improvement in heat and mass transfer obtained through the use of hybrid nanoparticles.

ARTICLE IN PRESS

Future Plan:

The present study demonstrates that magnetic fields significantly suppress fluid velocity, thermal radiation enhances temperature distribution, and the inclusion of Al_2O_3 - TiO_2 nanoparticles markedly improve heat transfer performance in Casson hybrid nanofluids. Activation energy effectively regulates mass transfer by moderating chemical reaction rates, while the close agreement between bvp4c and MWNN–PSO–NNA confirms the reliability of the proposed hybrid computational framework. These findings are directly applicable to industrial heat exchangers, lubrication systems, chemical processing units, and energy-efficient thermal management devices. Future work may extend the current model to unsteady flows, three-dimensional geometries, variable thermophysical properties, or experimental validation, as well as explore alternative intelligent algorithms for real-time prediction and control of complex nanofluid systems. Future research could

ARTICLE IN PRESS

expand the current MWNN–PSO–NNA model to handle transient, three-dimensional, and turbulent hybrid nanofluid flows. Enhancing the training dataset, exploring alternative hybrid ANN architectures, and incorporating experimental validation would further improve the model's robustness, generalization, and practical applicability.

Data Declarations

Data is provided within the manuscript.

Conflict of Interest

Authors declared no conflict of interest.

Ethical Approval

Not applicable

Funding

No funding.

Acknowledgement:

Not applicable

Authorship contribution statement

Mohammad Ayman-Mursaleen: Conceptualization, Investigation, Software

Syed Tauseef Saeed: Conceptualization, Investigation, Software, Project Administration, Supervision, Writing – original draft.

Saja Mohammad Almohammadi: Software, Validation, Writing – original draft.

Khalid Arif: Investigation, Methodology, Software

Muhammad Imran: Conceptualization, Investigation, Software, Project Administration

ARTICLE IN PRESS

9. References

1. Ghobadi, A. H., & Hassankolaei, M. G. (2019). A numerical approach for MHD Al2O3–TiO2/H2O hybrid nanofluids over a stretching cylinder under the impact of shape factor. *Heat Transfer—Asian Research*, *48*(8), 4262-4282.
2. Wu, X., & Zhao, Y. (2024). A Novel Heat Pulse Method in Determining "Effective" Thermal Properties in Frozen Soil. Water Resources Research, 60(12), e2024WR037537. doi: https://doi.org/10.1029/2024WR037537.

ARTICLE IN PRESS

3. Ai, C., Liu, C., Sun, P., & Liu, C. (2025). Na□CO□-SiO□-H□O nanofluids synergistically treats coal dust and hydrogen sulfide. Journal of Environmental Chemical Engineering, 13(6), 119365. doi: https://doi.org/10.1016/j.jece.2025.119365.
4. Induranga, A., Galpaya, C., Vithanage, V., Indupama, A., Maduwantha, K., Gunawardana, N., ... & Koswattage, K. (2025). Nanofluids for Heat Transfer: Advances in Thermo-Physical Properties, Theoretical Insights, and Engineering Applications. *Energies*, *18*(8), 1935.
5. Sharshir, S. W., Peng, G., Yang, N., Eltawil, M. A., Ali, M. K. A., & Kabeel, A. E. (2016). A hybrid desalination system using humidification-dehumidification and solar stills integrated with evacuated solar water heater. *Energy conversion and management*, *124*, 287-296.
6. Wu, Y., Du, X., Zhang, H. J., Wen, Z. F., & Jin, X. S. (2017). Experimental analysis of the mechanism of high-order polygonal wear of wheels of a high-speed train. *Journal of Zhejiang University-SCIENCE A, 18*(8), 579-592.
7. Lee, C. G., Hwang, Y. J., Choi, Y. M., Lee, J. K., Choi, C., & Oh, J. M. (2009). A study on the tribological characteristics of graphite nano lubricants. *International journal of precision engineering and manufacturing*, *10*(1), 85-90.
8. Ren, D., Wang, C., Wei, X., Zhang, Y., Han, S.,... Xu, W. (2025). Harmonizing physical and deep learning modeling: A computationally efficient and interpretable approach for property prediction. Scripta Materialia, 255, 116350.
9. Liu, Y., Wang, Y., Chen, S., & Zhang, J. (2025). A Novel Hybrid Neural Lyapunov Method with Low Conservatism for Power System Domain of Attraction Estimation. IEEE Transactions on Industrial Informatics, 21(7), 5580-5591.
10. Mei, W., Wang, X., Lu, Y., Yu, K., & Li, S. (2025). Learning and Current Prediction of PMSM Drive via Differential Neural Networks. IEEE Transactions on Circuits and Systems II: Express Briefs, 72(3), 489-493.
11. Kumar, M. D., Shah, N. A., Gurram, D., & Yook, S. J. (2025). Predicting thermal transport of blood-based penta-hybrid nanofluid in Fin geometries using deep neural networks and finite difference approach. Engineering Applications of Artificial Intelligence, 162, 112450.
12. Kumar, M. D., Shah, N. A., Dharmaiah, G., & Yook, S. J. (2025). Optimization and classification of thermal transport on a convective surface with non-uniformly shaped ternary hybrid nanofluid flows. Engineering Applications of Artificial Intelligence, 157, 111391.

ARTICLE IN PRESS

ARTICLE IN PRESS

13. Paul, A., Patgiri, B., & Sarma, N. (2025). Mixed convective flow of engine oil-based non-Newtonian tri-hybrid nanofluid across a porous rotating disk. *World Journal of Engineering*, *22*(3), 612-626.
14. Ayman-Mursaleen, M. Quadratic function preserving wavelet type Baskakov operators for enhanced function approximation. *Computational and Applied Mathematics*,*44(8),* 395 (2025).
15. Bhat, A. A., Khan, A. Boundary interpolation on triangles via neural network operators. *Mathematics Computer Simulation,* 241, 190-201 (2026).
16. Jiang, P., Zheng, H., Xiong, J., & Rabczuk, T. (2025). The localized radial basis function collocation method for dendritic solidification, solid phase sintering and wetting phenomenon based on phase field. Journal of Computational Physics, 520, 113515.
17. Bi, Y., Xia, G., Wang, C., Peng, M., Xu, Y.,... Wu, J. (2025). Design and transient analysis of a novel type passive residual heat removal system. Nuclear Engineering and Design, 445, 114446.
18. Liu, C., An, J., Nguyen, X. C., & Balasubramanian, P. (2025). Machine learning prediction of hydrochar adsorption capacity for methylene blue with limited data: Inspired by generative adversarial network-based augmentation. Energy & Environmental Sustainability, 1(4), 100043.
19. Tian, H., Yi, X., Zhang, Y., Wang, Z., Xi, X.,... Liu, J. (2025). Dynamical Analysis, Feedback Control Circuit Implementation, and Fixed-Time Sliding Mode Synchronization of a Novel 4D Chaotic System. Symmetry, 17(8), 1252.
20. Mei, W., Wang, X., Lu, Y., Yu, K., & Li, S. (2025). Learning and Current Prediction of PMSM Drive via Differential Neural Networks. IEEE Transactions on Circuits and Systems II: Express Briefs, 72(3), 489-493.
21. Wan, A., Du, C., AL-Bukhaiti, K., & Chen, P. (2025). Optimizing combined-cycle power plant operations using an LSTM-attention hybrid model for load forecasting. Journal of Mechanical Science and Technology. doi: 10.1007/s12206-025-0961-3.
22. Mohanty, D., Mahanta, G., Shaw, S., & Das, M. (2024). Thermosolutal Marangoni stagnation point GO–MoS2/water hybrid nanofluid over a stretching sheet with the inclined magnetic field. *International Journal of Modern Physics B, 38*(02), 2450024.
23. Mohanty, D., Mahanta, G., Chamkha, A. J., & Shaw, S. (2025). Numerical analysis of interfacial nanolayer thickness on Darcy-Forchheimer Casson hybrid nanofluid flow over a

ARTICLE IN PRESS

moving needle with Cattaneo-Christov dual flux. *Numerical Heat Transfer, Part A: Applications, 86*(3), 399-423.

24. Aslam, M.N., Ali, A., Junaid, M.S. *et al.* Machine learning-assisted thermal analysis of propylene glycol nanofluid with dual flux and bioconvection over a Riga plate. *Sci Rep* **15**, 35327 (2025).
25. Arif, K., Saeed, S.T., Aslam, M.N. *et al.* Modelling cross-diffusion in MHD Williamson nanofluid flow over a nonlinear stretching surface via Morlet wavelet neural networks. *Sci Rep* **15**, 27287 (2025).
26. Jameel, M., Shah, Z., Rooman, M., Alshehri, M. H., Vrinceanu, N., & Antonescu, E. (2024). Entropy driven optimization of non-linear radiative chemically reactive sutterby nanofluid flow in presence of gyrotactic micro-organism with Hall Effect and activation energy. *Scientific Reports, 14*(1), 30338.
27. Baithalu, R., Panda, S., Pattnaik, P. K., & Mishra, S. R. (2024). Entropy analysis in magnetized blood-based hybrid nanofluid flow via parallel disks. *Partial Differential Equations in Applied Mathematics, 12,* 100941.
28. Kumar, M., Kaswan, P., Kumari, M., Ahmad, H., & Askar, S. (2024). Cattano Christov double diffusion model for third grade nanofluid flow over a stretching Riga plate with entropy generation analysis. *Heliyon, 10*(10).
29. Kaswan, P., Kumar, M., Kumari, M., & Öztop, H. F. (2025). Thermal analysis of hybridized AA7072 and AA7075 alloys nanomaterials within MHD Darcy-Forchheimer flow through a moving thin needle. *Thermal Advances, 2,* 100020.
30. Agrawal, R., Saini, S. K., & Kaswan, P. (2025). Analysis of bidirectional flow of Williamson micropolar fluid in porous medium with activation energy and thermal radiation. *Numerical Heat Transfer, Part B: Fundamentals, 86*(2), 262-287.
31. Panda, S., Ontela, S., Mishra, S. R., & Thumma, T. (2024). Effect of Arrhenius activation energy on two-phase nanofluid flow and heat transport inside a circular segment with convective boundary conditions: Optimization and sensitivity analysis. *International Journal of Modern Physics B, 38*(25), 2450342.
32. Shamshuddin, M. D., Salawu, S. O., Panda, S., Mishra, S. R., Alanazy, A., & Eid, M. R. (2024). Thermal case exploration of electromagnetic radiative tri-hybrid nanofluid flow in Bi-directional stretching device in absorbent medium: SQLM analysis. *Case Studies in Thermal Engineering, 60*, 104734.

ARTICLE IN PRESS

ARTICLE IN PRESS

33. Panda, S., Pradhan, G., Nayak, D., Pattnaik, P. K., & Mishra, S. R. (2024). Presentation of entropy due to heat transfer irreversibility of MHD Williamson fluid over an inclined channel. *Modern Physics Letters B, 38*(07), 2450010.
34. Nabwey, H. A., Jakeer, S., Mansour, M. A., Salah, T., & Rashad, A. M. (2025). Entropy generation on MHD hybrid nanofluid flow over a porous square cavity with a cross-shaped obstacle and heater corners. *Journal of Thermal Analysis and Calorimetry, 150*(22), 18405-18428.
35. Jakeer, S., Grace, D. S., Durgaprasad, P., Reddy, S. R. R., & Basha, H. T. (2025). Two-phase Carreau bio-magnetic hybrid nanofluid flow over an inclined spinning disk: numerical simulation and machine learning. *Multiscale and Multidisciplinary Modeling, Experiments and Design, 8*(8), 355.
36. Jakeer, S., Reddy, S. R. R., Thameem Basha, H., Cho, J., & Sathishkumar, V. E. (2025). Activation energy and Coriolis force impact on three-dimensional dusty nanofluid flow containing gyrotactic microorganisms: Machine learning and numerical approach. *Nanotechnology Reviews, 14*(1), 20250179.
37. Awais, M., Soomro, F. A., Khokhar, R. B., & El-Sapa, S. (2024). Heat transfer augmentation through engine oil-based hybrid nanofluid inside a trapezoid cavity. *Mehran University Research Journal Of Engineering & Technology*, *43*(1), 24-33.
38. Sarma, N., & Paul, A. (2024). Engine oil blended Casson hybrid nanofluid flow along a uniformly heated curved surface with Arrhenius activation energy and suction: a computational study. *Hybrid Advances*, *5*, 100161.
39. Mohanty, D., Mahanta, G., Chamkha, A. J., & Shaw, S. (2025). Numerical analysis of interfacial nanolayer thickness on Darcy-Forchheimer Casson hybrid nanofluid flow over a moving needle with Cattaneo-Christov dual flux. *Numerical Heat Transfer, Part A: Applications*, *86*(3), 399-423.
40. Reddy, M. V., Nath, J. M., Ali, F., Das, T. K., Khan, U., & Garayev, M. (2025). Implementation of homotopy analysis method for entropy-optimized two-phase nanofluid flow in a bioconvective non-Newtonian model with thermal radiation. Journal of Radiation Research and Applied Sciences, 18(1), 101218.
41. Malik, M. F., Aljethi, R. A., Shah, S. A. A., & Yasmeen, S. (2025). Hybrid Nanofluid Flow and Heat Transfer in Inclined Porous Cylinders: A Coupled ANN and Numerical Investigation of MHD and Radiation Effects. Symmetry, 17(11), 1998.

ARTICLE IN PRESS

ARTICLE IN PRESS

42. Ullah, K., Ullah, H., Fiza, M., Jan, A. U., Akgül, A., Hendy, A. S., ... & Khan, I. (2025). Neural network analysis of ternary hybrid nanofluid flow with Darcy-Forchheimer effects. Journal of Radiation Research and Applied Sciences, 18(2), 101362.
43. Qureshi, H., Shah, Z., Khan, W. A., Hassaballa, A. A., Shatat, A., & Muhammad, T. (2025). Machine learning investigation with neural network modelling for Sutterby Multi-hybrid fluid in biomedical treatments. Results in Engineering, 25, 104427.
44. Saeed, S. T., Arif, K., & Qayyum, M. (2024). Exact solutions of non-singularized MHD Casson fluid with ramped conditions: A comparative study. *Advances in Mechanical Engineering, 16*(8), 16878132241272170.
45. Shehzad, S. A., Hayat, T., Qasim, M., & Asghar, S. (2013). Effects of mass transfer on MHD flow of Casson fluid with chemical reaction and suction. *Brazilian journal of chemical engineering, 30,* 187-195.
46. Ullah, M. E., Idrees, M., Saeed, S.T., and Zubaidi, A.A. Prandtl ternary nanofluid flow with magnetohydrodynamics and thermal effects over a 3D stretching surface using convective boundary conditions. *ZAMM□Journal of Applied Mathematics and Mechanics*, 105 (5): e70078, 2025.
47. Zahmani, Q. F., Asmuin, N., Sued, M. K., Mokhtar, S. N. A., & Sahar, M. N. H. (2024). Nanofluid-Infused Microchannel Heat Sinks: Comparative Study of Al_2O_3, TiO_2, and CuO to Optimized Thermal Efficiency. *Journal of Advanced Research in Micro and Nano Engineering*, *19*(1), 1-12.
48. Dhamecha, B. D., Popat, H. M., & Makadia, J. J. (2014). Heat Transfer Enhancement Using Nano Fluid-A Review. *International Journal of Engineering Research & Technology, 3*(1), 2702-2705.
49. Ghadikolaei, S. S., & Gholinia, M. (2020). 3D mixed convection MHD flow of GO-MoS2 hybrid nanoparticles in H2O–(CH2OH) 2 hybrid base fluid under the effect of H2 bond. *International Communications in Heat and Mass Transfer*, *110*, 104371.
50. Ghadikolaei, S. S., Gholinia, M., Hoseini, M. E., & Ganji, D. D. (2019). Natural convection MHD flow due to MoS2–Ag nanoparticles suspended in C2H6O2H2O hybrid base fluid with thermal radiation. *Journal of the Taiwan Institute of Chemical Engineers*, *97*, 12-23.
51. Imran, M., Jia, W., Saeed, S.T. *et al.* AI-powered prediction of hybrid nanofluid dynamics over a cylinder via LM optimized neural network approach. *Sci Rep* **15**, 37217 (2025).

ARTICLE IN PRESS

ARTICLE IN PRESS

52. Uddin, Z., Upreti, H., Ganga, S., & Ibrahim, W. (2024). Particle Swarm Optimization for exploring Darcy–Forchheimer flow of Casson fluid between co-axial rotating disks with the Cattaneo–Christov model. *Scientific Reports*, *14*(1), 7891.
53. Yatim, H. M., Mohd-Ghazali, N., Mohamad, M., Pamitran, A. S., & Novianto, S. (2023). Two-phase heat transfer microchannel system identification with Particle Swarm Optimization (PSO) approach. *International Journal of Air-Conditioning and Refrigeration*, *31*(1), 13.
54. Imran, M., Saeed, S.T., Younis, J. *et al.* ANN-based thermal analysis of 3D MHD hybrid nanofluid flow over a shrinking sheet via LMA. *Sci Rep* **15**, 33137 (2025).
55. Iliyasu, A. M., Benselama, A. S., Bagaudinovna, D. K., Roshani, G. H., & S. Salama, A. (2023). Using particle swarm optimization and artificial intelligence to select the appropriate characteristics to determine volume fraction in two-phase flows. *Fractal and Fractional*, *7*(4), 283.
56. Syah, R., Elveny, M., Nasution, M. K., Ponkratov, V. V., Kuznetsova, M. Y., Poltarykhin, A. L., & Babanezhad, M. (2021). Numerical investigation of nanofluid flow using CFD and fuzzy-based particle swarm optimization. *Scientific Reports*, *11*(1), 20973.
57. Khurana, D., Yadav, A., & Sadollah, A. (2023). A non-dominated sorting based multi-objective neural network algorithm. *MethodsX*, *10*, 102152.
58. Tekir, M. (2025). Experimental study on the thermal performance of hybrid nanofluid in a compact plate heat exchanger under the influence of a magnetic field. *Case Studies in Thermal Engineering, 69,* 106031.
59. Sahin, F., & Namli, L. (2023). Experimental investigation of heat transfer characteristics of magnetic nanofluids (MNFs) under a specially designed revolving magnetic field effect. *Journal of Magnetism and Magnetic Materials, 580,* 170961.

ARTICLE IN PRESS